University of Trento

Department of Industrial Engineering

Mechanical Design for Mechatronics

professor Emiliano Rustighi

Technical report

Optimization of a Massage Gun

Assirelli Alessandro,
Bottene Alessandro,
Govindarajan Karthik,
Perini Marco,
Vogric Sanja

December 2021

Contents

1 Abstract **2**

2 Introduction **2**

3 Product Design Specification **3**
3.1 Quality Function Deployment 5

4 Design Process **6**
4.1 Function Decomposition 6
4.2 Linear Motion 6
4.2.1 Mechanical Reciprocating Motion Mechanisms 6
4.3 Rotary motion 7

5 Final Design Proposal **8**
5.1 Material Selection 9

6 Preliminary Design **10**
6.1 Model and Optimization 10
6.2 Electrical Motor 11

7 Device Analysis and verification **12**
7.1 Follower 13
7.2 Rod End Connector 13
7.3 Rod 15
7.4 Connecting Rod Pin 16
7.5 Bushing 17
7.6 Eccentric Motor Hub 17
7.7 Bearings 18
7.7.1 Bearing Selection 18
7.7.2 Single row deep groove ball bearing - 6001-2RSL 19
7.7.3 Angular contact bearing-double row - 3200 A-2RS1TN9/MT33 21
7.8 Barrel Cam 24

8 Product Review **26**

9 Conclusions and Annexes **27**

1 Abstract

The purpose of this report is the realization of a 2 - degrees of freedom (DoF) massage gun for medical and rehabilitation purposes. It is based on a reciprocating motion mechanism that can be achieved using different techniques presented in this document. The second DoF is given by the rotation of the head around its axis. Our objective is to implement the rotation and design a prototype with improved overall performances.

2 Introduction

Massage guns, also known as percussion massagers, percussive therapy, and vibration therapy, aim to reduce inflammation by flushing extracellular fluids such as lymph fluid and venous blood out of the muscle tissues and into the circulatory system. It can help relax tight muscles, break up scar tissue and adhesions, and minimize muscle soreness (preventing DOMS[1]) and tension.

Workout and race recovery have always been crucial for a good athletic performance. Nowadays there is a vast variety of methods and tools that focus on muscle relieving. Between them, massage guns rose in popularity due to their simple design, user-friendliness and accessibility. The reciprocating motion of the head relaxes the muscles and increases blood and lymphatic circulation. The advantages of this kind of massagers go beyond the initial stress relieving. They can help prepare the body for future performances by improving flexibility and mobility, encouraging healing and preventing injuries. In the end, also the overall wellness of the user can be positively affected. Many athletes indeed reported improvements in sleep and a general reduction of stress.

Since massage guns started being available on the market, they became an indispensable aid for more and more athletes. Despite that, not many changes have been made to improve their performances. We believe that the benefits of massage guns can be enhanced by adding a rotatory motion to the head. With this added degree of freedom, the head will be able to follow the natural line of the muscles, more likely to what physiotherapist do, which may improve muscle relaxation ad flexibility.

[1] Delayed onset muscle soreness

3 Product Design Specification

Studying commercially available mechanisms, we focused our attention on the main requirements our 2-DOF massage gun should have. The aim is to realize a percussive massager with improved overall performances and a tunable rotation profile. Taking into account the best features of different models, we want to obtain:

- High frequency
- High stall force
- Compact chassis
- User friendliness

An overview of all the request (R) and desires (D) of the 2 - DoF massage gun is schematically represented in Table 1.

Geometry		
Maximum dimensions	300x 200 x 80	D
Weight	< 1 kg	R
Kinematics		
Frequency	≥ 3000 ppm	R
Easy head substitution		R
Head rotation		R
Head translation	$12 - 16$ mm	R
Tunable rotation profile		D
Energy		
Electric powered		R
Battery life	> 3 h	D
Charging time	≈ 2 h	D
Dynamics		
Stall force	$300 - 400$ N	D
Low internal inertia		D
Balanced forces		D
Materials		
Corrosion resistance		R
Hypoallergenic head		R
Scratch resistance	medium	R
Vibration absorbing		R
Waterproof casing	$\geq$ IP65	D
Finishes		
Components standardisation	high	R
Components from outside suppliers		R
Number of components	limited	D
Mounting	easy	D
Charging USB port		D
Terms of use		
Fiction coefficient between sliding surfaces	low	D
Wear	low	D
Noise level	low	D
Easy to use	high	R
Safe to use	high	D
Expected lifetime	1000 h	R
Assembly/disassembly	easy	D
Insensitive to vibrations		D
Ergonomics and aesthetics		
Easy to handle		R
Handle diameter	4 - 5 cm	D
Interchangeable battery		D

Table 1: Product Design Specification

3.1 Quality Function Deployment

In order to envision our desires and requirements we utilized the quality function deployment table (QFD), which it is represented in Figure 1. The customer's requests are in the rows and they are correlated with the specifications in the columns, like it is shown in the correlation legend. On top of the main QFD table, there are reported the reciprocal influences between the specifications as described in the influence legend. Finally on the left side four potential costumers categories are compared with the requirements, by assigning a score from 1 to 10, based on the importance of the requests.

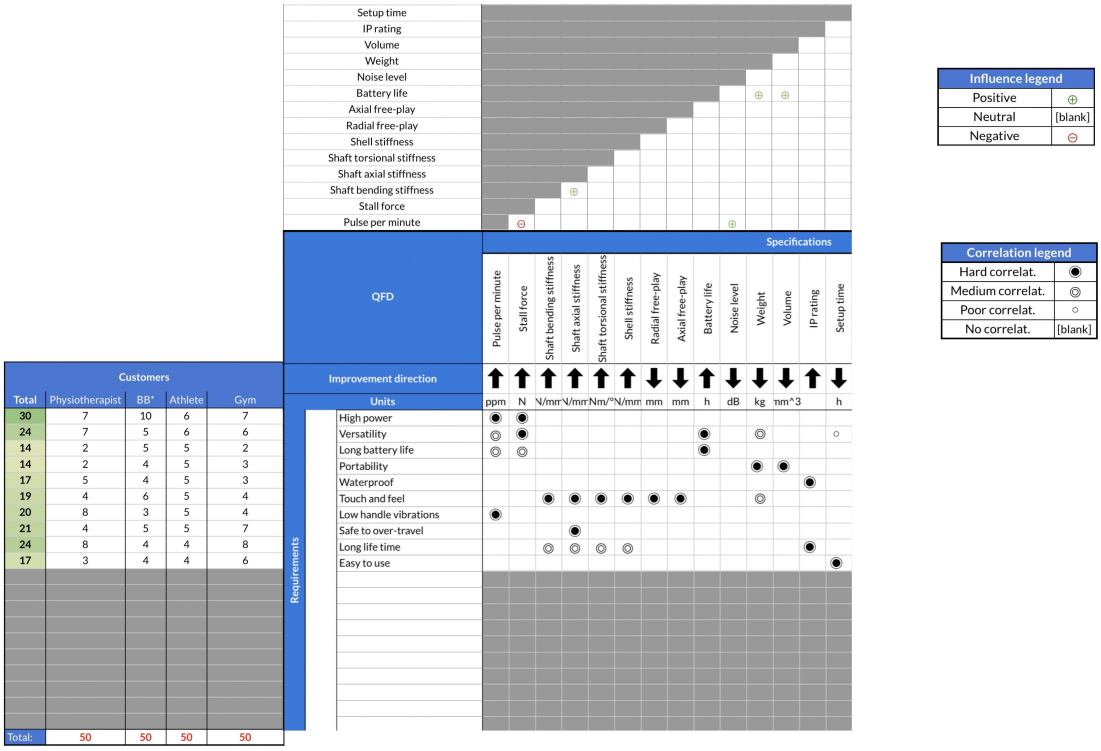

Figure 1
QFD

4 Design Process

4.1 Function Decomposition

To better approach the design of the massage gun, we split the functional relationships into their constituent parts. The flow chart represented in Figure 2 was the starting point for the future analysis.

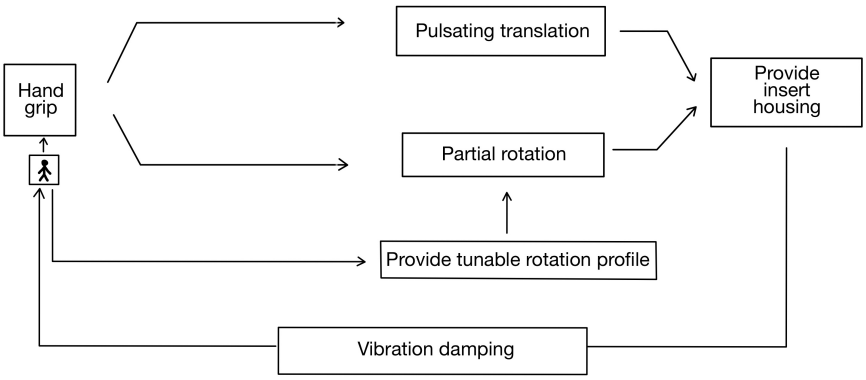

Figure 2
Function decomposition scheme

Among these functions we mainly focused on providing linear and rotational motion, which are the core of this massage gun.

4.2 Linear Motion

We analyzed different types of commercially available linear actuators, comparing them to find the right one that meets the product design specification.

Electric based

- Linear servo motor
- Linear induction motor
- Rotary Electric Motors with leadscrew
- Rotary Electric Motors with Reciprocating Mechanisms

Pneumatic/Hydraulic

- Tie-rod cylinders

4.2.1 Mechanical Reciprocating Motion Mechanisms

When using a rotary electric motor, we should consider different types of reciprocating mechanisms that convert the rotational motion into a periodic linear one.

The most common are:

- Slider-crank
- Camshaft
- Scotch Yoke (slotted link)

- Swashplate (slant disk)

After a first selection of the most relevant linear motion actuators, we picked the most promising ones an compared them. They were given a score from one to five for each of the desired properties. After evaluating the total scores, the slider-crank and the camshaft mechanisms were the ones which could give the best performances. In the end the camshaft was not selected due to its limitations regarding noise and wear, making the slider-crank the adopted linear motion mechanism.

4.3 Rotary motion

To realize the rotation we chose to focus on a barrel cam mechanism. It consists of a cylindrical cam with grooves, in which the follower can slide. Among many possible options, we chose the case in which the follower is a cylinder as well. For this particular configuration, the interaction between follower and cam is made possible by the means of a cylindrical pin which is attached to the follower's surface. The pin glides in the barrel cam channel, following its path as seen in Figure 3. In our case the cam (in green) should be fixed to the frame, which will give the follower (in blue) the freedom to translate and rotate around its axis. Furthermore, to obtain a tunable rotation profile the cam should be removable and interchangeable with other cams. The groove should be designed to provide different profiles of rotation to the head.

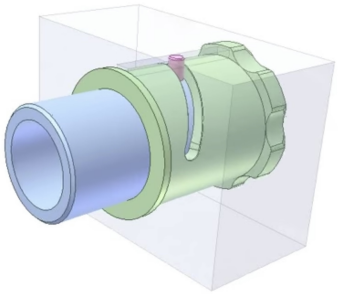

Figure 3
Representation of a barrel cam with a cylindrical follower

5 Final Design Proposal

Taking into account all the previous considerations we have made, we opted to use an electric motor together with a slider-crank mechanism to achieve the reciprocating motion and a barrel cam for the rotation of the head attachment. A brushless DC motor is used to provide enough torque as well as a minimum number of revolutions per minute, connected to the rod by an eccentric hub. The rod is jointed on the other side to the rod connector, which is then connected to the follower with a bearing that allows rotation. The follower is equipped with three pins to follow the grooves on the cam and it's able to slide forth and back, while rotating in the so called cylindrical cam. The cam (gear) is connected to the case with a thread, which makes it interchangeable. By changing the gear it's possible to select different rotation profiles according to the need, of course the gear with straight grooves would realize the typical motion of massage guns.

Finally we set the maximum force $F_{max} = 350\ N$, maximum pulse per minute $n_{max} = 4000\ rpm$ and the maximum stroke $s = 12\ mm$.

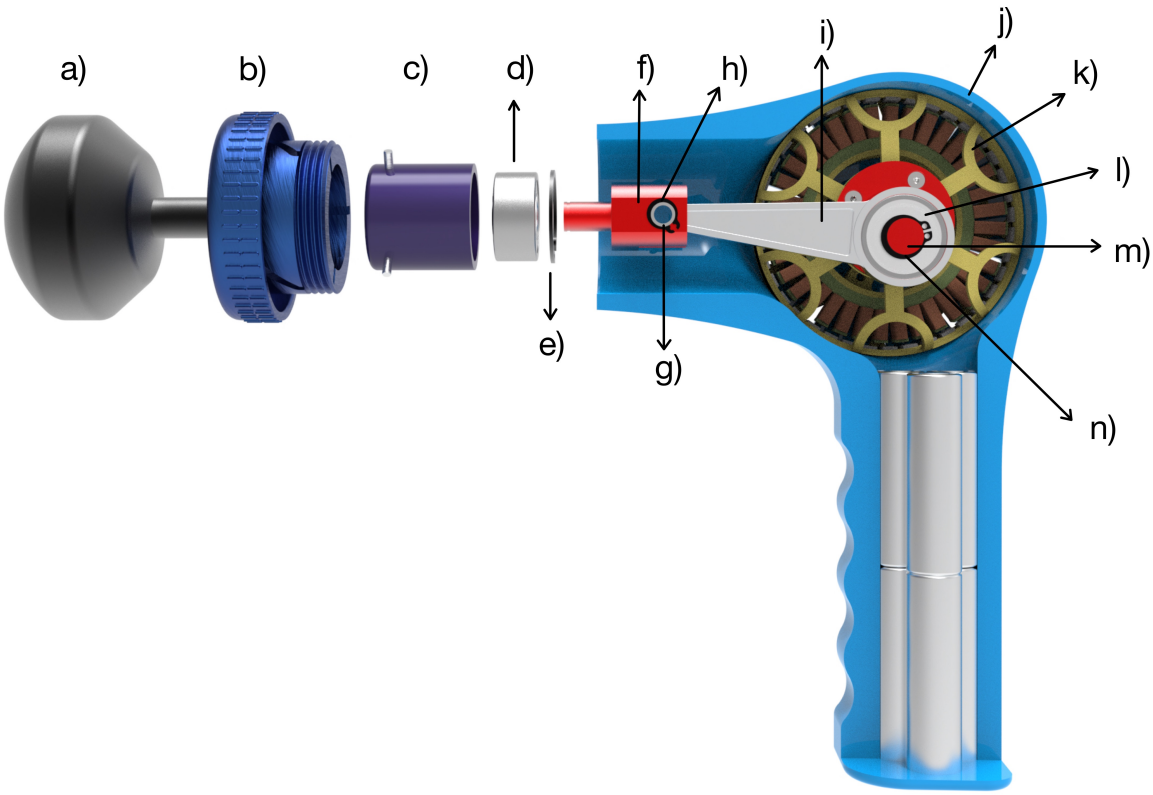

Figure 4
Exploded-view drawing of the final design proposal:
a) Head; b) Barrel cam; c) Piston/ Follower with pins UNI EN ISO 8734 - 3x10;
d) Bearing 2: 3200 A-2RS1TN9/MT33; e) Seeger DIN 472 - 30x1.2; f) Rod connector;
g) Connecting rod pin; h) Seeger DIN 471 - 8x0.8 i) Rod; j) Casing; k) Electric motor;
l) Bearing 1: 6001 - 2RSL ; m) Eccentric hub/ Motor interface; n) Seeger DIN 471 - 12x1

5.1 Material Selection

For the design of the 2-DOF massage gun each material was chosen to satisfy specific functional requests, but overall, all of the parts described in this section, have to satisfy a low density requirement. The massage gun, in fact, has to be easy to handle and lightweight.

- **Rod, Connector, Follower and Pins**

Al was chosen to realize the follower and the pins, because of its low density and good performances in contact with PA 6. Among the variety of **Al** alloys, **6061** is the one exhibiting the best compromise between forgeability and strength. It is an Al - Mg - Si alloy, with low alloying content, than can be solution heat treated after its manufacturing.

	ρ g/cm^3	σ_y Mpa	**E** GPa	ν /
Al 6061	2.70	276	68.9	0.33

Table 2: Density, yield strength, Young modulus and Poisson modulus of Al 6061

- **Barrel cam**

The main requirement for the barrel cam material is to have a low friction coefficient with respect to the follower. Because of its good tribological properties Nylon 6, also known as **PA 6**, was considered. This material is characterised by a low density, satisfactory toughness, impact resistance and high chemical resistance.

	ρ g/cm^3	σ_y Mpa	**E** GPa	ν /	μ_s steel /	μ_d Al /
PA 6	1.10	100	4.20	0.39	0.3	0.06

Table 3: Density, yield strength, Young modulus and Poisson modulus of PA 6

- **Casing and Head**

Casing and head need respectively a high toughness and fatigue resistance. This is why polypropylene (**PP**) can be a potential candidate for their design. In addition to having a really low density, it possesses a good thermal and chemical stability and it is overall easy to produce and manufacture.

	ρ g/cm^3	σ_y Mpa	**E** GPa	ν /
PP	0.92	45.0	1.68	0.42

Table 4: Density, yield strength, Young modulus and Poisson modulus of PP

6 Preliminary Design

6.1 Model and Optimization

A model of the sliding movement is developed in MapleSim environment. All the joints are treated as ideal and the CoM for each link is considered in the mid-point of the bar. As a first stage, we used rough estimations of bars weight and inertia, the masses were then constantly updated for each iteration with the development of the CAD model. The rotational component is not considered here and its calculations are provided in Section 7.8.

The first challenge was finding the torques required to provide the target output force at the end-effector. To address this problem we modeled the motor as a constant velocity source, leaving the torque as an unknown. Then the contact force is modeled as a constant force acting on the third bar, as shown in Figure 5a. This approximation differs from the reality by the fact that the contact force is not constant, since the muscle

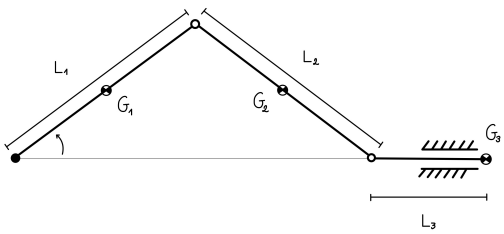

(a) Slider crank model

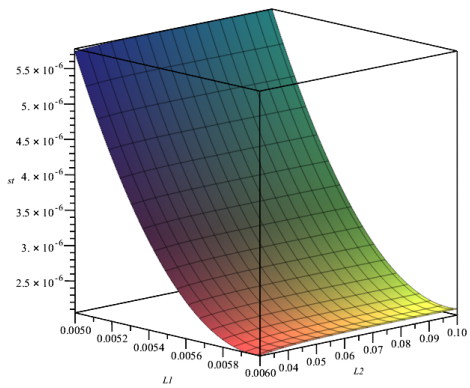

(b) Cost function used in optimization

tissues have a spring-damper behaviour and because the force is acting only when the gun is in the pushing phase. Since we were interested in an estimation of the maximum required torque this approximation works fine.

The model was then used to tune the parameters of the mechanism. This problem is known as synthesis of a mechanism. In our case we had just two parameters to optimize: L_1 and L_2, the two lengths of the bars. The cost function we used tries to minimize the difference between the desired stroke ($S_{des} = 12[mm]$) and minimizing the input torque required to satisfy our force requirement:

$$\min_{L_1,L_2} \alpha|s_{des} - s|^2 + \beta|\tau|^2$$
$$\text{subject to } M(q)\ddot{q} + h(q,\dot{q}) = \tau$$

where α and β are weighting factors, s is the stroke, τ is the maximum torque.

In Figure 5b is shown the cost function. As can be seen there is very little dependence on L_2, this is because the stroke, which has a much greater importance, depends only on L_1, while the combination of L_1 and L_2 determines the torque, which has less importance. Moreover looking at the static conditions L_2 plays no role, and so its importance is very limited. Even though for this specific case we didn't get much from these results, we thought it is a nice approach to design mechanisms, and so it has been presented. The MapleSim and Maple files used can be found in appendix. The final lengths were then approximated to get rounded values: $L_1 = 6\ mm$, $L_2 = 80\ mm$.

6.2 Electrical Motor

According to the specification and the results of the simulation we have two main requirements for the motor: $\tau \geq 2.5\ Nm$ and $n \geq 3200\ rpm$. We opted for the EaglePower 8308-KV180.

Specification	Value
Power	1200 W
Nominal voltage	22.2 V
KV	180
Dimensions	93x28.5 mm
Weight	336 g

Table 5: EaglePower 8308-KV180 specifications

We can get the maximum torque dividing P by ω.

$$\omega = \frac{Voltage \cdot KV \cdot 2\pi}{60} = 420\ rad/s = 3996\ rpm$$
$$\tau = K_s \cdot \frac{P}{\omega} = 2.85\ Nm$$

The service factor K_s is set to one because we considered the power as the maximum power that the motor can provide. The torque, and thus the maximum force, in the real product would be regulated by some electric circuit. This is needed for safety reasons, indeed the maximum amount of force when working with an old patient must be less then the one needed for an athlete.

7 Device Analysis and verification

To model a real-case use of the system, we introduced a combination of an axial and a radial forces applied to the head attachment. For simplicity we will consider the case with straight, vertical grooves, in this way there isn't any contribution force by pins. The presence of a cylindrical constraint on the follower is modeled as a distributed reaction force. The structure is analyzed on X-Z and Y-Z planes, note that, as can be seen in Figure 8, on X-Z plane the mechanism is 1-time hyperstatic. The full analysis was carried out in Maple and it can be found in the attachment. Here we report the main results along with the static verification. To cross check the results we also performed a simple FEM analysis, obtained by simulating the whole mechanism. An accurate FEM analysis was not the scope of the course, nor of the project, so it is presented just to show the similarities with our study.
We considered the worst case ($\theta_m = 90$); the values of the reaction forces are reported in Table 6.

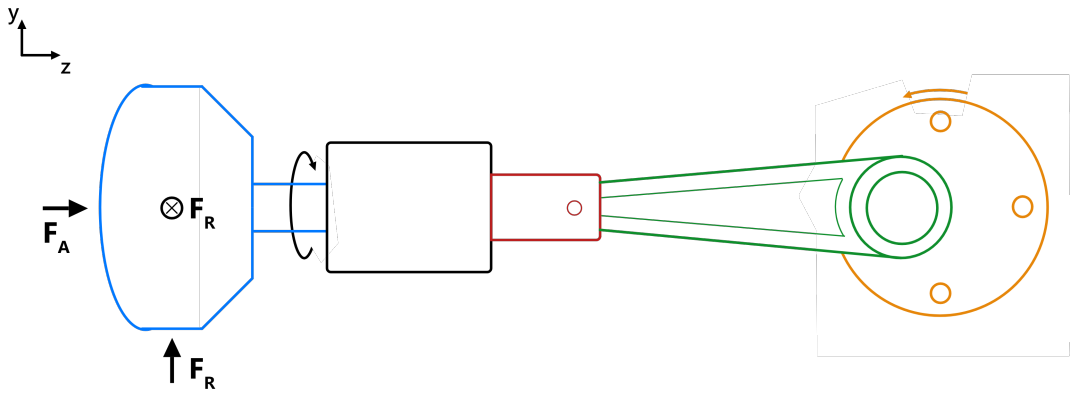

Figure 6
Styled mechanism

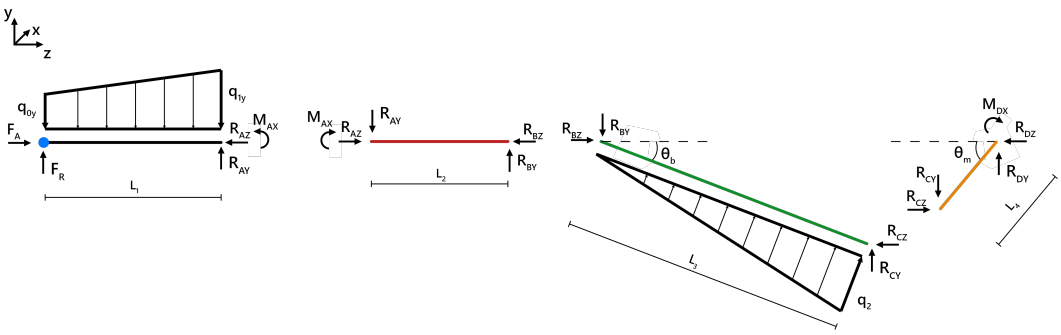

Figure 7
Mechanism FBD y-z plane

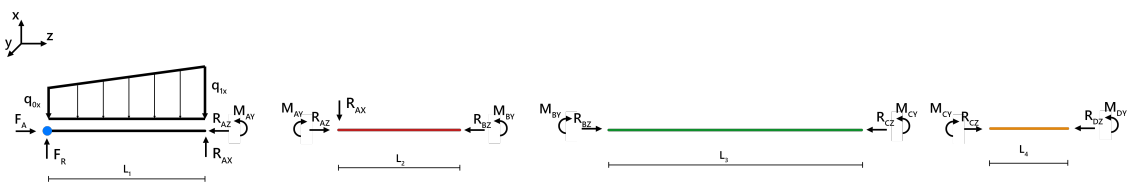

Figure 8
Mechanism FBD x-z plane

Follower	Connector	Rod	Hub
rax = 0			
ray = 27.7	rby = 27.7	rcy = = 23.6	rdy = = 23.6
raz = 350 N	rbz = 350 N	rcz = 350.3 N	rdz = 350.3 N
may = -184.9 Nmm	mby = -184.9 Nmm	mcy = -184.9 Nmm	mdy= -184.9 Nmm
max = 692.4 Nmm			mdx = 2101.8 Nmm
q0x = 7.7 N/mm			
q1x = -4 N/mm			
q0y = 6.2 N/mm			
q1y = -1.7 N/mm			
L1 = 100 mm	L2 = 25 mm	L3 = 80 mm	L4 = 6 mm

Table 6: Reaction forces

7.1 Follower

The analysis is carried out on the most critical section, at $z = 25mm$ where we have the maximum bending moments in both x-z and y-z planes.

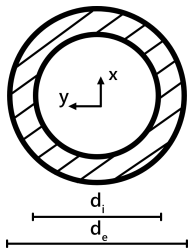

Figure 9
Most critical section

$$\sigma_{max} = \frac{M_{xmax}}{I_{xx}} \cdot \frac{d_e}{2} - \frac{M_{ymax}}{I_{yy}} \cdot \frac{d_e}{2} = 1.67\ MPa$$

7.2 Rod End Connector

Since we want the follower to be able to rotate, we need to decouple this degree of freedom from the alternating sliding motion imposed by the slider-crank mechanism. We introduce a component linked to the rod with a connecting pin, while the top is inserted in the inner ring of an angular contact bearing. This permits the transmission of the axial sliding motion, while allowing also the rotation of the outer ring fixed to the follower.

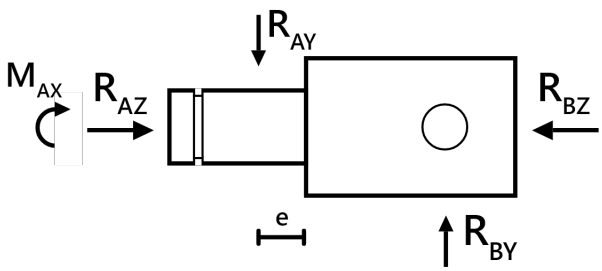

Figure 10
Connector top view

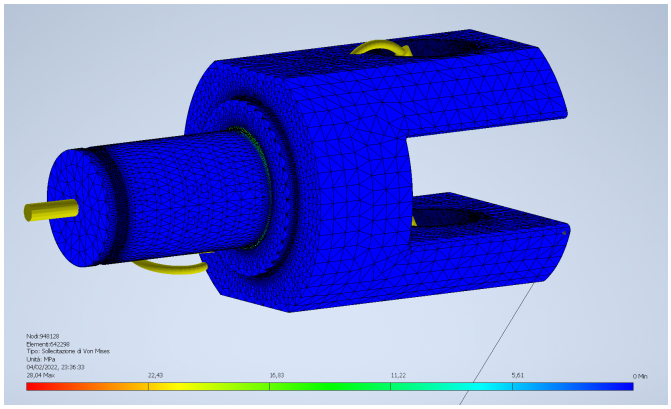

Figure 12
Rod connector FEM

The verification takes into account bending moments on both axes.

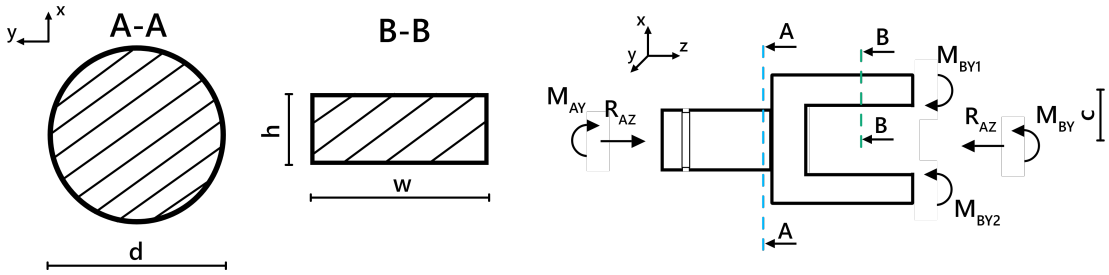

Figure 11
Most critical sections

The first critical section analysed is

$$\sigma_{A-A_{max}} = \frac{(M_{A_x} - R_{A_y} \cdot e)}{I_{xx_{A-A}}} \cdot \frac{d}{2} - \frac{M_{A_y}}{I_{yy_{A-A}}} \cdot \frac{d}{2} = 7\ MPa$$

$$\sigma_{B-B_{max}} = \frac{(M_{A_y} - R_{A_z} \cdot c)}{I_{xx_{B-B}}} \cdot \frac{h}{2} = 5.7\ MPa$$

Around B-B section, the part could be subject to crushing, we must make sure that the shear on the internal surface of the hole is less than:

$$\frac{350\ N}{2} \leq \frac{\sigma_{R,Al6061} \cdot d_{hole} \cdot t}{phi} = \frac{305\ MPa \cdot 8\ mm \cdot 5.5\ mm \cdot 2}{2} = 13420\ N$$

7.3 Rod

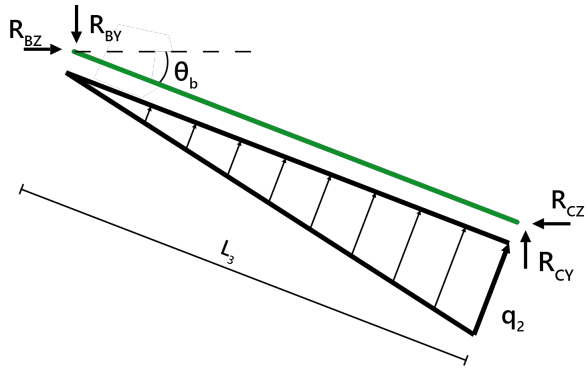

Figure 13: Rod FBD

First, a pre-dimensioning is carried out using Euler's buckling formula,

$$I_0 = \frac{\mu \cdot F_{max} \cdot L_0^2}{\pi \cdot E^2}$$

Where L_0 is the unsupported length, F_{max} the maximum axial force, E the Elastic modulus and μ a pre-dimensioning coefficient which for combustion engines varies from 10-20. A first value of the moment of inertia of the section I_0 is obtained. Once established the shape and therefore the relations between the main length h and other dimensions of the section, it is possible to find the minimum h_{min} value which satisfies the equation.
We fix a safety coefficient of 5 for the maximum admissible stress, and we consider in the calcuation of $\lambda = \frac{L0}{r}$ the worst unsupported length $(L0 = 1 \cdot L)$ by XZ and YZ plane
The section is now verified with Rankine's formula,

$$N_{max} = \frac{\sigma_{am} \cdot A}{1 + \alpha \cdot \lambda^2} = \frac{\frac{305}{5}\ MPa \cdot 21.49\ mm^2}{1 + \alpha \cdot \lambda^2} = 759.9\ N$$

Where

$$\alpha = \frac{2 \cdot \sigma_{amm}}{\pi^2 \cdot E} = \frac{2 \cdot 61\ MPa}{\pi^2 \cdot 69000\ MPa} = 0.00017$$

The component is verified for buckling as long as $N < N_{max}$:

$$\phi = \frac{N_{max}}{N_{rod}} \approx 2$$

In our case we adopted *h=6.5 mm* to guarantee a safety factor of 2 on critical buckling load.

The next verification is carried out with the crank-rod mechanism in motion, at 90°, where other than the axial load, there is a centrifugal force acting on the I-beam,

$$F_c = m \cdot \omega^2 \cdot r$$

This force can be modeled as a distributed load:

$$q_i = \rho \cdot A_f \cdot \frac{x}{L} \cdot \omega^2 \cdot r$$

Maximum bending moment is found where the shear is zero, in $x = \frac{L}{\sqrt{3}}$. A first verification is carried in this point using values of internal actions obtained from the analysis provided in the Appendix.

$$\sigma_m = \frac{Mx \cdot y_{max}}{I_{yy}} + \frac{My \cdot x_{max}}{I_{xx}} = \frac{52\ Nmm \cdot 6.780\ mm}{34.696\ mm^4} + \frac{185\ Nmm \cdot 2.438\ mm}{714.639\ mm^4} = 10.8\ MPa$$

This has to be added to the normal stress:

$$\sigma_a = \frac{N_{rod}}{A_f} = \frac{351\ N}{32.565\ mm^2} = 10.8\ MPa$$

The resulting total stress is way lower than the yield strength of Al6061.

$$\sigma_t = \sigma_a + \sigma_m = 17.35 << 276\ MPa$$

Another important zone for verification is around the small end, where we find the lowest cross-section

$$\sigma_m = \frac{10\ Nmm \cdot 3.373\ mm}{32.258\ mm^4} + \frac{185\ Nmm \cdot 2.438\ mm}{112.756\ mm^4} = 5.04\ MPa$$
$$\sigma_a = \frac{350\ N}{0.997 \cdot 21.49\ mm^2} = 16.34\ MPa$$

Due to difficulties in modeling the notch behaviour in the two different planes, we rely on FEM analysis to better define the stress in this area.

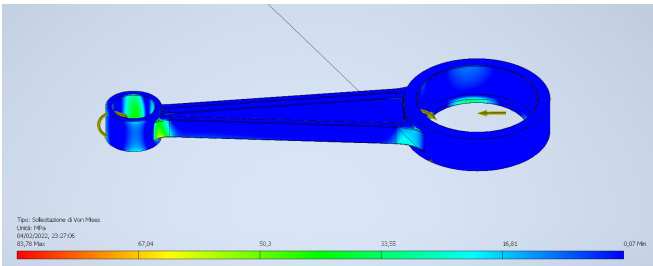

Figure 14
Rod FEM

7.4 Connecting Rod Pin

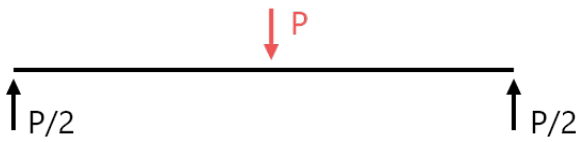

Figure 15
Pin free body diagram

The connecting Rod pin is modeled as a beam suspended over two sliders, which represent the piston housing for the pin, and subject to a central load P, which would be the axial force acting on the Rod. L is considered as the distance between piston housing centers. Since the pin cannot be considered as a thin beam ($\frac{L}{h} > 10$), we just focus on the shear stress.

$$T_{max} = \frac{P}{2} = \frac{351\ N}{2} = 175.5\ N$$

Pin has a hollow circular section cylinder, therefore the shear stress, and the consequent Von-Mises stresses are:

$$\tau = 2 \cdot \frac{T_{max}}{\pi \cdot R \cdot b} = 2 \cdot \frac{175.5\ N}{\pi \cdot 3\ mm \cdot 2\ mm} = 9.3\ MPa$$
$$\sigma_{VonMises} = \sqrt{3 \cdot \tau^2} = \sqrt{3 \cdot 9.3^2} = 16.13\ MPa$$

The total VM stress is much lower than the yield strength of 100Cr6 steel of 835 MPa. We have chosen such a large diameter for the pin, mainly because of the life-span of the composite bushing, which lies in the rod small end.

7.5 Bushing

An intermediate component is needed in the rod small-end to house the connecting pin. Since the space is quite limited, we opted for a composite bushing. It has been chosen using SKF Bearing Selector (see Appendix), given the data of our condition which are:

Specification	Value
d_{max}	8 mm
Radial force	0.351 kN
Frequency	4000 rpm
Half oscillation angle	4.3 °
Temperature	30 °C
Roughness	0.4 μm

Table 7: Specifications for bushing dimensioning

Since we need a bushing able to withstand an important load, for its dimensions, we opted for the best alternative, with the highest basic load rating. This POM composite bushing consists of a sheet steel backing on which a 0,2 to 0,4 mm thick layer of tin/bronze is sintered.
Again, an extra polyoxymethylene (POM) layer, with a thickness of approximately 0,25 to 0,45 mm is firmly attached to the sintered tin/bronze layer and has pockets to retain grease.

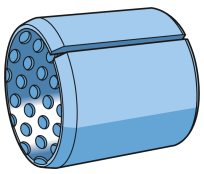

Figure 16
POM Bushing

Although the life expectancy of the bushing could increase if periodically lubricated, in our case the initial lubrication could be enough since the sliding surface contains grease reservoirs, and the location of the component is not subject to the presence of contaminating elements.

7.6 Eccentric Motor Hub

According to the Model Optimization results, the best length for the crank is $L_2 = 6.0\ mm$.
To achieve this very little length, considering also the tiny available space, the best outcome was to design an eccentric hub, bolted directly on the outrunner motor cage with four M3 bolts. The hub is simply made

of a turned cylinder, with a face in contact with the motor outer case, and an eccentric cylinder of diameter $d = 6.0\ mm$. This diameter has been chosen mainly to fit the bearing lifetime requirements.

Since the motor comes with M3 screws, we only do the verification for the hub, without considering the fastening. Here the pin is considered as a beam.

The axial load comes from bending:

$$\sigma_a = \frac{M_{Dy}}{I_{xx}} \cdot \frac{d}{2} = \frac{184.9Nmm}{1017.8mm^4} \cdot \frac{12mm}{2} = 1MPa \tag{1}$$

The shear load is equivalent to the normal load acting on the rod; using Jourawsky:

$$\tau = \frac{4}{3} \cdot \frac{N_{rod}}{\pi r^2} = 4.13MPa \tag{2}$$

The verification is satisfied since:

$$\sqrt{3\tau^2 + \sigma_a^2} = 3.7Mpa << 276MPa \tag{3}$$

Looking at the FEM analysis we observe a strong difference in Von Mises equivalent stress; a possible reason could be that the beam assumption is not valid here.

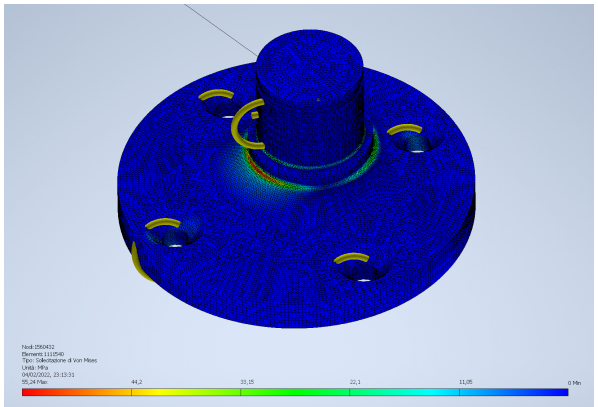

Figure 17
Motor Hub FEM

7.7 Bearings

In our slider-crank mechanism we use an electric motor to provide the required force to the massage head. Between the crank and the rod we need an element to allow rotation and withstand the radial load. Due to high loads and high speeds we decided to use a radial bearing. We will then refer to this as B1 (bearing 1).

The follower which is sliding in the cylindrical cam grooves, has the freedom to translate and rotate around its axis. The torque from the electric motor gets transferred towards the follower-cam axis by a slider-crank mechanism. To allow the rotation of the massage head, we decided to fit a bearing between the connecting rod and the follower, which is then directly connected to the massage head. We will refer to this as B2 (bearing 2).

7.7.1 Bearing Selection

The choice for B1 was easy due to the standard application that it has to accomplish. For the second bearing we considered: thrust bearings, radial bearings, angular contact, angular contact double row bearings and combined needle roller bearings. Thrust bearings were discarded because the small ones can only transfer unidirectional loads. Even though there are also bidirectional ones, they are too big and in both cases the housing design becomes complicated. Deep groove bearings are not recommended to work with axial loads

higher than 25% of the radial one. Combined needle roller bearings fulfil the load conditions, but the size and weight factor lead to more changes in the overall design of the product. Angular contact bearings are a trade-off between these three categories. We decided for an angular contact double row bearing since it can deal with bidirectional axial load while, at the same time, simplifying the housing design.

7.7.2 Single row deep groove ball bearing - 6001-2RSL

Deep groove ball bearings are the most widely used bearing type and are particularly versatile. In our conditions we require a bearing which can accommodate high rotational speed and radial load carrying capacity.

Among the available designs we chose the single row deep groove ball bearing -6001-2RSL which is a standard variant that comes without filling slots. This bearing fulfills the loading requirements and the dimension requirement.

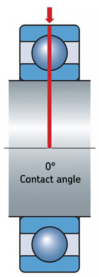

Figure 18
Radial Loading direction - B1

The maximum load conditions for the radial bearing are shown in Table 8 . In our case the speed of the electric motor is considered constant.

Conditions	Value
Radial Load (F_r)	0.35kN
Axial Load (F_a)	0kN
Speed (n)	4000 rpm
Inner ring- Temperature °C	40°C
Outer ring- Temperature °C	40°C

Table 8: Main input data and parameters (B1)

B1 is not loaded with any axial load. Due to the above condition the equivalent dynamic load P and equivalent static load P_o are the same.

$$P_o = F_r$$
$$P = F_r \Rightarrow 0.35\ kN$$
$$\frac{C}{P} = \frac{5.4\ kN}{0.35\ kN} \Rightarrow 12.86$$

The influence of permanent deformation on bearing performance is described by the static safety factor S_o.

$$S_o = (\frac{C_o}{P_o}) \Rightarrow (\frac{2.36\ kN}{0.35\ kN}) = 5.62$$

Bearings capped on both sides are lubricated for the life of the bearing and are virtually maintenance-free. We have chosen LHT23 standard bearing lubricant from the technical specifications of SKF standards. Inner ring temperature ranges from 30°C to 40°C and the same for outer ring. The actual viscosity ν is 26.9 mm^2/s, while viscosity ratio k is 2.01. Low viscosity ratio $k < 1$ will lead to reduced asperity contact; on the other hand $k > 4$ leads to an increase of bearing rating life, but results in higher viscous frictional losses. In the traffic light concept of Figure 21b there is the temperature range for each grease.

To keep the bearing lubricated and avoid external contamination a sealing system is required. Low-friction seals provide better sealing effectiveness than non-contact seals and are made of sheet steel reinforced NBR (oil- and wear-resistant). RSL design make virtually no contact, allowing higher speeds as it is shown in Figure 19.

Selection guidelines for SKF capping devices

Requirement	Shields	Non-contact seals	Low-friction seals		Contact seals	
	Z, ZS	RZ	RSL	RST	RSH	RS1
Low friction	+++	+++	++	++	∘	∘
High speed	+++	+++	+++	+	∘	∘
Grease retention	∘	+	+++	+++	+++	++
Dust exclusion	∘	+	++	++	+++	+++
Water exclusion						
static	–	–	∘	+++	+++	++
dynamic	–	–	∘	+	++	+
high pressure	–	–	∘	∘	+++	∘
Symbols:	+++ = best	++ = very good	+ = good	∘ = fair	– = not recommended	

Figure 19
Selection guideline for sealings.

The minimum radial load that must be provided to let the bearing work properly is:

$$F_{r,m} = K_r(\frac{\nu \cdot n}{1000})^{2/3}(\frac{d_m}{100})^2$$
$$d_m = 0.5(D+d) \Rightarrow 0.5(28+12) = 20\ mm$$
$$F_{r,m} = 0.025(\frac{26.9 \cdot (4000)}{1000})^{2/3}(\frac{20}{100})^2 \Rightarrow 0.023\ kN$$

This load is easily obtained by the rod and by interference of the housing. Since the load on this bearing is acting on the outer ring, we selected interference fit for the housing and loose fit for the hub. This choice is based on SKF recommendations; it provides an easy way to mount the bearing on the shaft, and a proper working of the bearing. Interference fit of the housing provides both preload and axial locking. Since only interference usually is not enough to have a proper axial constraint we also use a seeger. The tolerances for housing and shaft are picked from the producer recommendations: N7/g6.

Duty intervals with constant bearing load P and speed n can maintain the bearing life. In our case the

speed n is constant, so the life is expressed in operating hours using L_{10_h}.

$$L_{10} = (\frac{C}{P})^p$$
$$L_{10} = 3673.7\ h$$
$$L_{10_h} = (\frac{10^6}{60(4000)}) \cdot L_{10}$$
$$L_{10_h} = (4.17) \cdot 3673.7 \Rightarrow 15306\ h$$

where L_{10} = basic rating life [millions of revolutions](at 90% reliability), L_{10_h} = basic rating life [operating hours] (at 90% reliability), p = exponent of the life equation equal to 3 for ball bearings.

7.7.3 Angular contact bearing-double row - 3200 A-2RS1TN9/MT33

Angular contact ball bearings have inner and outer ring raceways that are displaced relative to each other in the direction of the bearing axis. The axial load carrying capacity of angular contact ball bearings increases as the contact angle increases.

This can also be achieved by two single row angular contact ball bearings arranged back-to-back, but with an increase in weight. The contact angle of 25° has reduced sensitivity to axial loading and misalignment while accommodating two times higher impact loads.

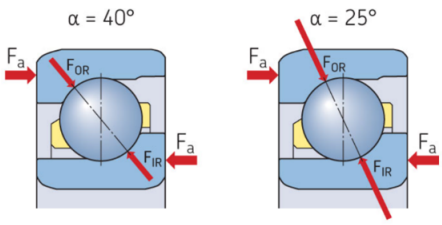

Figure 20
Contact angle difference for angular contact bearing

Different contact angles are available, within the range of 25°, 30°, 40°, 45°. Increasing the contact angle improves axial load carrying capacity, by trading off radial load carrying capacity. Axial internal clearance of bearings in the series 32 A has the C2 clearance class. We opted for t 3200 A-2RS1TN9/MT33 (suffix explanation in Table 9 as B2, as it fulfils the loading conditions. Values in the Table 10 are the operational input feed for the B2.

Abbreviation	Meaning
2RS1	Contact seal, NBR, on both sides
MT33	Medium temperature grease
TN9	Glass fiber reinforced PA66 cage

Table 9: Bearing suffix codes abbreviation

The maximum axial load acting on B2 is equal to the maximum axial load of the gun ($FA = 350N$). The maximum radial load is obtained by considering the combination of $rax = 27.7N$ and $ray = 0N$, so the total radial load is equal to rax. This configuration was considered for the most critical conditions for the bearing, because it involves both axial and radial load. The minimum load $F_{r,m}$ which has to be maintained for the bearing is 52N, which is achieved by the preload. Maximum load conditions for bearing B2 are reported in Table 10.

Conditions for Case-2	Value
Radial Load (F_r)	0.052 KN
Axial Load (F_a)	0.35 KN
Speed (n)	1000 rpm
Inner ring- Temperature °C	40°C
Outer ring- Temperature °C	40°C

Table 10: Case-2 input data and parameters (B2)

The equivalent dynamic bearing load P is obtained by multiplying the axial and radial loads by their respective factors Y and X:

$$\frac{F_a}{F_r} > e \Rightarrow P = X \cdot F_r + Y_2 \cdot F_a$$

$$P = 0.63 \cdot (0.052) + 1.24 \cdot (0.35) \Rightarrow 0.47\ kN$$

When the load ratio $\frac{C}{P} > 10$, the operating temperature is below 100 °C (210 °F) and the operating speed is below 50% of the limiting speed, this indicates the bearing is operating under a safe region. For us the load ratio is:

$$\frac{C}{P} = \frac{7.61}{0.47} \Rightarrow 16.3$$

The static safety factor S_o for B2 is:

$$S_o = (\frac{C_o}{P_o}) \Rightarrow (\frac{4.3}{0.283}) = 15.2$$

To lubricate the bearing we decided to use the provided MT33 lubricant, which comes with the SKF angular contact double row bearings. As can be seen in Figure 21a and Figure 21b MT33 satisfies the requirements.

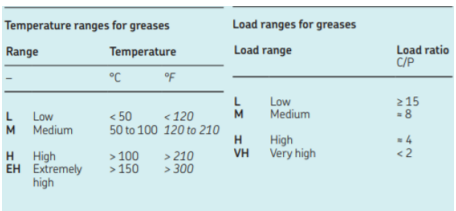

Temperature ranges for greases

Range		Temperature	
–		°C	°F
L	Low	< 50	< 120
M	Medium	50 to 100	120 to 210
H	High	> 100	> 210
EH	Extremely high	> 150	> 300

Load ranges for greases

Load range		Load ratio C/P
L	Low	≥ 15
M	Medium	≈ 8
H	High	≈ 4
VH	Very high	< 2

(a)
Temperature and load range for grease

Technical specifications of SKF standard and special greases for capped deep groove ball bearings

Grease	Temperature range[1]	Thickener	Base oil type	NLGI grade	Base oil viscosity [mm²/s] at 40 °C (105 °F)	at 100 °C (210 °F)	Grease performance factor (GPF)
MT33		Lithium soap	Mineral	3	100	10	1
MT47		Lithium soap	Mineral	2	70	7,3	1
LT10		Lithium soap	Diester	2	12	3,3	2
LHT23		Lithium soap	Ester	2–3	27	5,1	2
LT		Lithium soap	Diester	2	15	3,7	1
WT		Polyurea	Ester	2–3	70	9,4	4
GJN		Polyurea	Mineral	2	115	12,2	2
HT		Polyurea	Mineral	2–3	96	10,5	2
VT378		Aluminium complex soap	PAO	2	150	15,5	–[1]
GFJ		Aluminium complex soap	Synthetic hydro-carbon	2	100	14	1
GE2		Lithium soap	Synthetic	2	25	4,9	2

(b)
Traffic light concept from SKF

Figure 21: Grease selection guide

The minimum load $F_{r,m}$ which has to be achieved is:

$$F_{r,m} = K_r(\frac{\nu \cdot n}{1000})^{2/3}(\frac{d_m}{100})^2$$

$$d_m = 0.5(D+d) \Rightarrow 0.5(30+10) = 20\ mm$$

$$F_{r,m} = 0.06(\frac{99.9 \cdot (1000)}{1000})^{2/3}(\frac{20}{100})^2 \Rightarrow 0.052\ kN$$

In our case the speed n is constant, so the bearing life can be expressed in operating hours using L_{10_h}.

$$L_{10} = (\frac{C}{P})^p$$
$$L_{10} = 4330h$$
$$L_{10_h} = (\frac{10^6}{60 \cdot (1000)}) \cdot L_{10}$$
$$L_{10_h} = (16.67) \cdot 4330 \Rightarrow 72193\ h$$

where L_{10} = basic rating life [millions of revolutions] (at 90% reliability), L_{10_h} = basic rating life [operating hours] (at 90% reliability), p = exponent of the life equation = 3 for ball bearings.

Since the load on this bearing is acting on the inner ring, we selected interference fit for the hub. Interference fit provides the necessary preload to fulfill the minimum radial load $F_{r,m}$ requirement and prevents the slipping of the inner ring. The tolerances for shaft are picked under the producer recommendations: js5.

Since the recommended tolerances are only given for steel or cast iron housings we had to estimate the interference for the nylon seat of B2 that is needed to prevent slipping. Indeed the contact pressure is strongly related to the elastic modulus E, which for nylon is about 50 times smaller than steel and thus a specific analysis is required. Here are presented the calculations that lead to the definition of the interference for the outer ring of the bearing.

First we impose the condition to avoid slipping and then we find the pressure needed to satisfy the condition:

$$F_{radial} = \frac{F_{axial}}{\mu^2} = 133.33\ N$$
$$p_{min} = \frac{F_{axial}}{2\pi r_{ext} B}\phi_{slip} = 0.1\ MPa$$

Please note that F_{axial} is not the maximum axial force that the gun is able to provide when it's pushing against the muscles. That force can't provide any slip because of the shoulder on the housing. In this case $F_{axial} = 35\ N$ is the maximum axial force acting in the opposite direction, which takes into account the inertia of the mechanism in the pulling phase. We can use the following formula that relates the pressure to the interference:

$$p = \frac{\delta}{\frac{d}{E_o}(\frac{d^2+d_o^2}{d_o^2-d^2} + \nu_o) + \frac{d}{E_i}(\frac{d_i^2+d^2}{d^2-d_i^2} - \nu_i)} \tag{4}$$

By using the materials' properties defined before, and remembering that the outer material is Nylon, while the inner is steel, we get the minimum diametrical interference $\delta_{min} = 0.0022\ mm$. The upper bound for interference is instead dictated by the yielding of the plastic piston. We can get the pressure that leads to yield with the following formula:

$$\frac{\sigma_y}{\phi_y} \leq p_{max}\frac{d_o^2 + d^2}{d_o^2 - d^2} + p_{max} \tag{5}$$

Solving for p_{max} we get $p_{max} \approx 20\ MPa$. Now we can substitute in the previous equation to get the maximum δ, which is $\delta_{max} = 0.168\ mm$. The required tolerance is thus M6

7.8 Barrel Cam

In Chapter 4.3 concerning the rotary motion, we discussed the barrel cam mechanism with a cylindrical follower. For our purposes we decided to focus on a cam with three helical grooves and consequently a follower with three press-fitted pins.

To design the helical grooves we adopted a simple approach that consists in unrolling the surface of the cylindrical cam obtaining a rectangle. After drawing a straight line with a certain angle α, as shown in the Figure 22, we obtained the relationship between the α and γ, which is the angle of rotation of the head that we want to achieve. Considering l as the length of the cylindrical cam and r as its radius, the equation can be written as:

$$tan\alpha = \frac{\gamma r}{l}$$

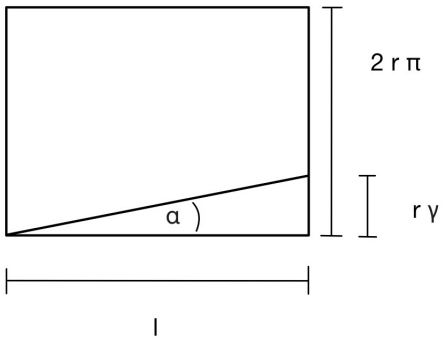

Figure 22
Schematic representation of an unrolled surface of a cylindrical cam

For our purposes we decided on a rotational angle γ of 30°. The mean radius r of the barrel cam is 22 *mm*, and the length in the axial direction dedicated to the grooves l is 12 *mm*. The resulting angle α is:

$$\alpha = arctan\frac{\gamma r}{l} \approx 44^\circ$$

The sliding of the pin in the helical grooves has a negative impact on the final force perceived by the user. Analyzing the situation for a single pin, as represented in the Figure 23, we can see how the force parallel to the cam channels P has a lower modulus than the force for the linear motion given by the motor T. This is due to the fact that during its translation, the follower is forced to follow the helical shape of the cam channels. Their curvature permits the rotation of the internal cylinder, but at the same time it is responsible for the existence of a component of F, which is perpendicular to the internal surface of the cam grooves N. The channels are assumed to be wide enough so that the sliding during the reciprocating motion is only on one out of the two surfaces. Taking into account that α is the helical angle, we can write the following relationships:

$$P = Fcos\alpha$$
$$N = Fsin\alpha = Ptan\alpha$$

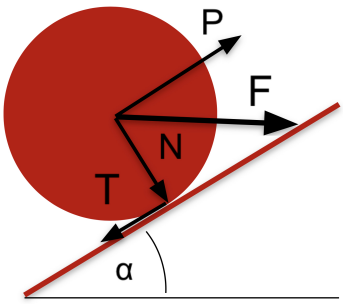

Figure 23
Schematization of a cylindrical pin sliding in a helical groove

The normal force N is responsible for the generation of a frictional force T between the channels and the pin. T and N are related by the means of the frictional coefficient μ. To calculate the final force given to the head F_{TOT}, we have to vectorially sum P and T. The calculation is reported in the steps below:

$$T = \mu N = \mu P tan\alpha$$
$$F_{TOT} = P - T = P(1 - \mu tan\alpha)$$

This simplified approach does not take into account the existence of multiple cam channels, in other words multiple pins on the follower. In the case of three axisymmetric pins, the force F given by the motor is equally distributed on each pin. Considering that the forces on each pin are $\frac{1}{3}$ of the total force and F_{TOT} is the sum of the forces in the groove direction calculated for each pin, the formula above remains unchanged.

In our case the force given by the motor F is $350N$. Therefore the F_{TOT} is:

$$F_{TOT} = F cos(\alpha)(1 - \mu tan\alpha) = 237\ N$$

This means we lose about 32 % of F_{TOT} because of the rotation.

8 Product Review

Some difficulties were encountered during the designing process of our 2-DoF massage gun.

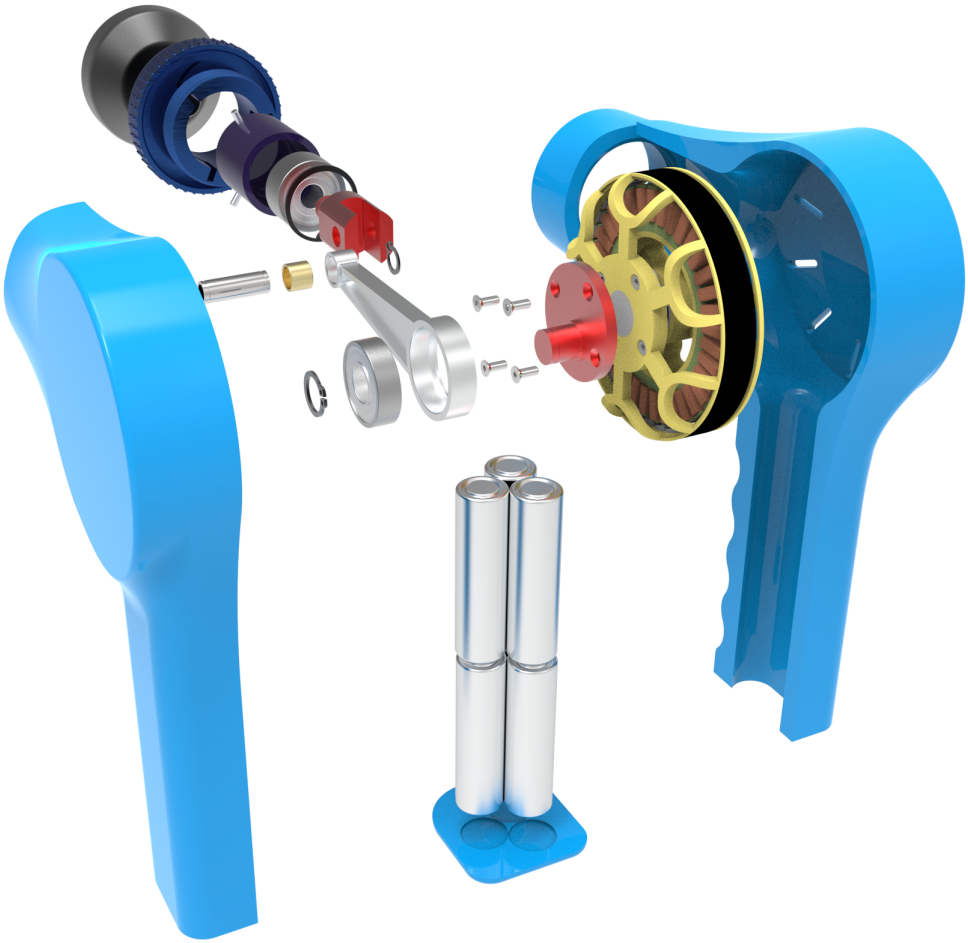

Figure 24
Exploded view of the final concept

For the rod verification, we considered the members' inertia, adding a centrifugal force as a distributed load on the rod. This simplified model is close to the real one and helpful for the calculations. To further improve the performance of the mechanism, we could have added some balancing weights on the motor shaft.

The angular contact bearing comes with M33 lubricant that is more suitable to work above 40 degrees, achievable after some time the gun is up and running. To work under those temperatures it would be better to use a custom lubricant.

Due to size limitations in the axial direction, it is hard to achieve noticeable rotation with the barrel cam without experiencing a great loss in force due to groove orientation and friction. Nevertheless, it is possible to achieve better performances by optimizing the grooves' shapes, getting custom velocity and acceleration profiles.

Our aim was to design a massage gun that can be commercialized. Where we could, we opted for standardized components, like in the cases of the pin, bearings and seeger - circlips. In addition to this, there are still some design considerations that have to be done to lower the overall cost of the product.

9 Conclusions and Annexes

We managed to design our 2-DoF massage gun from scratch, improving overall performances and meeting the initial requirements. Where possible we have used standard components in order to ease the manufacturing processes needed to bring our product to the market. Although some aspects can still be improved, we are very happy with the results and how the teamwork ended up.

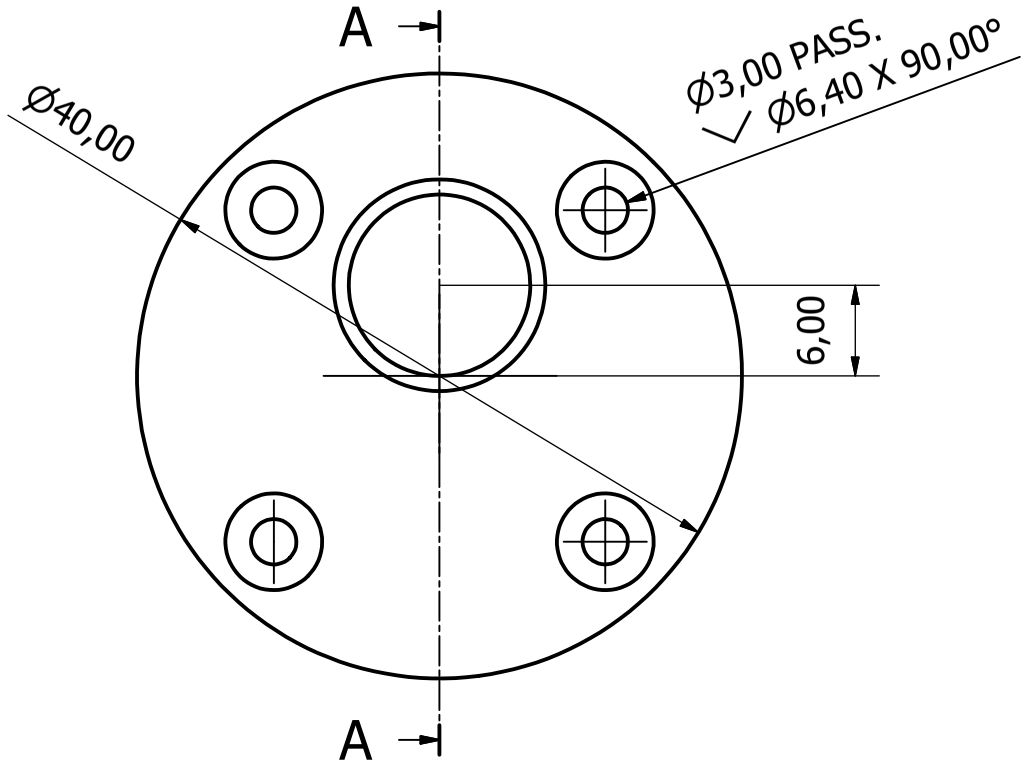

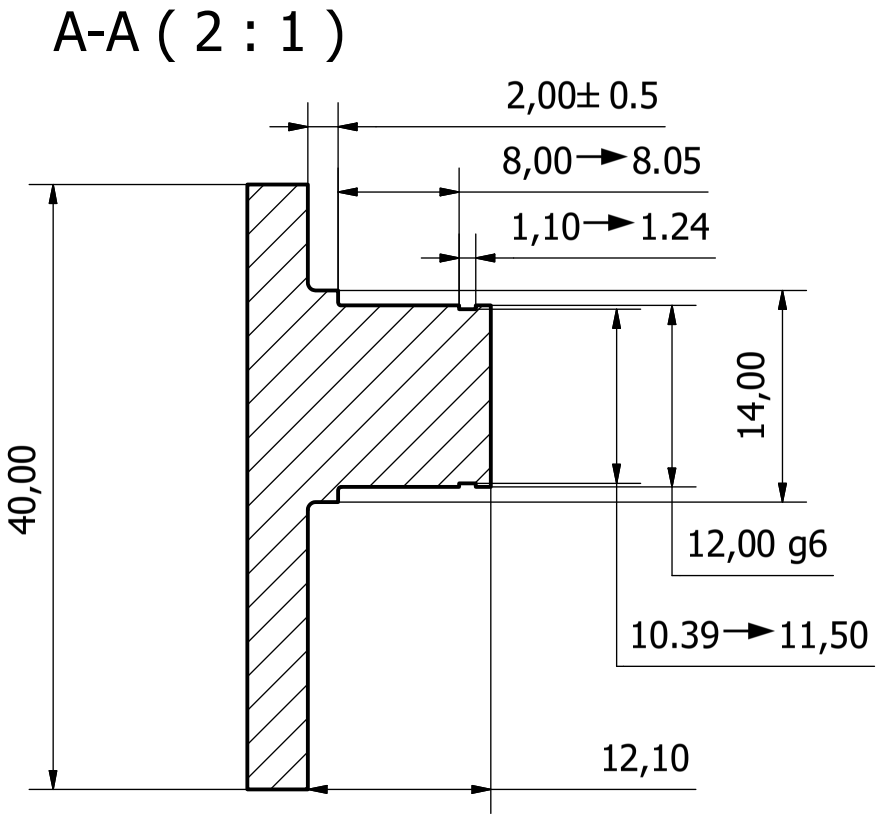

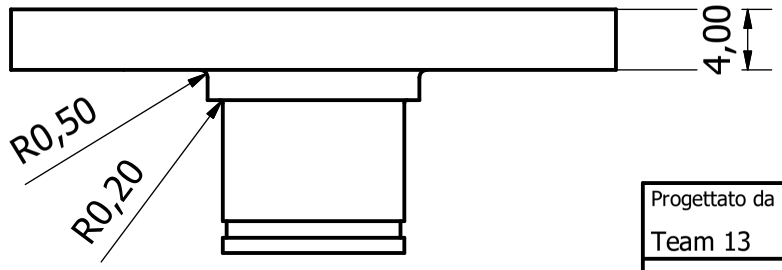

Progettato da	Controllato da	Approvato da	Data		Data	
Team 13					03/01/2022	
Interface between motor and 6001 bearing				motor interface	Edizione	Scala 2:1

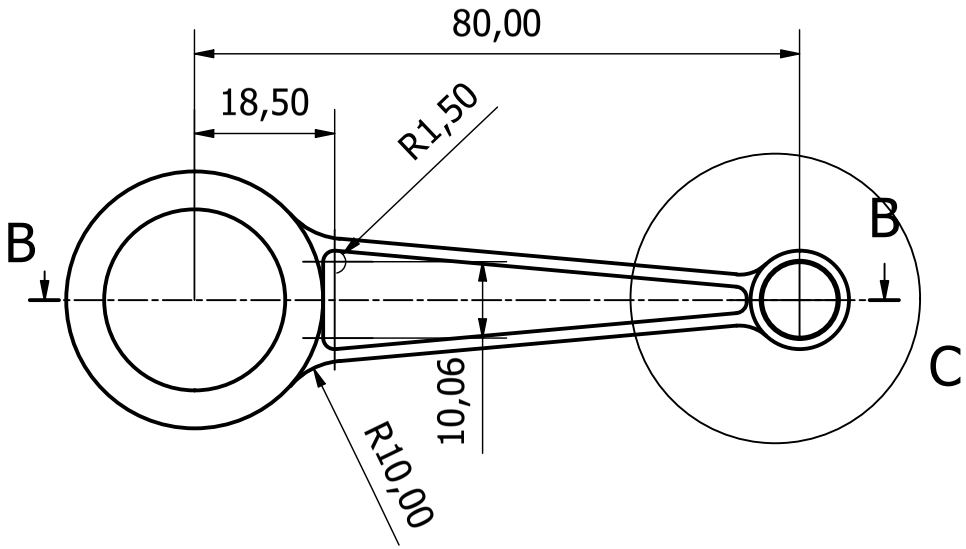

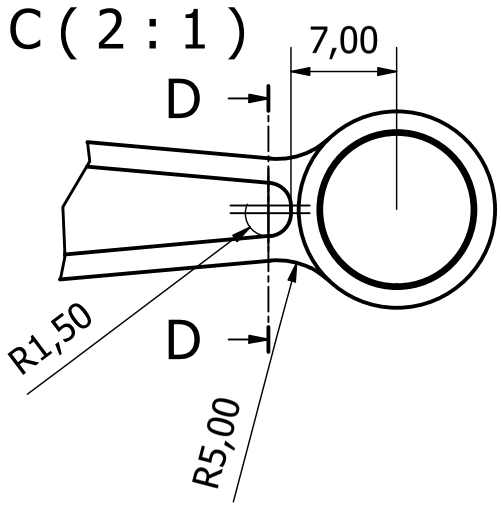

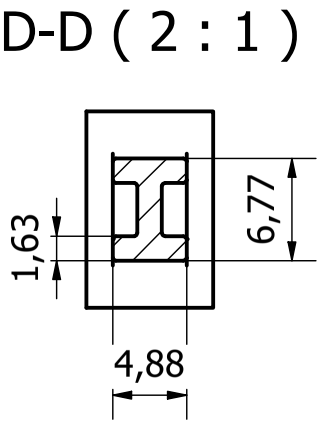

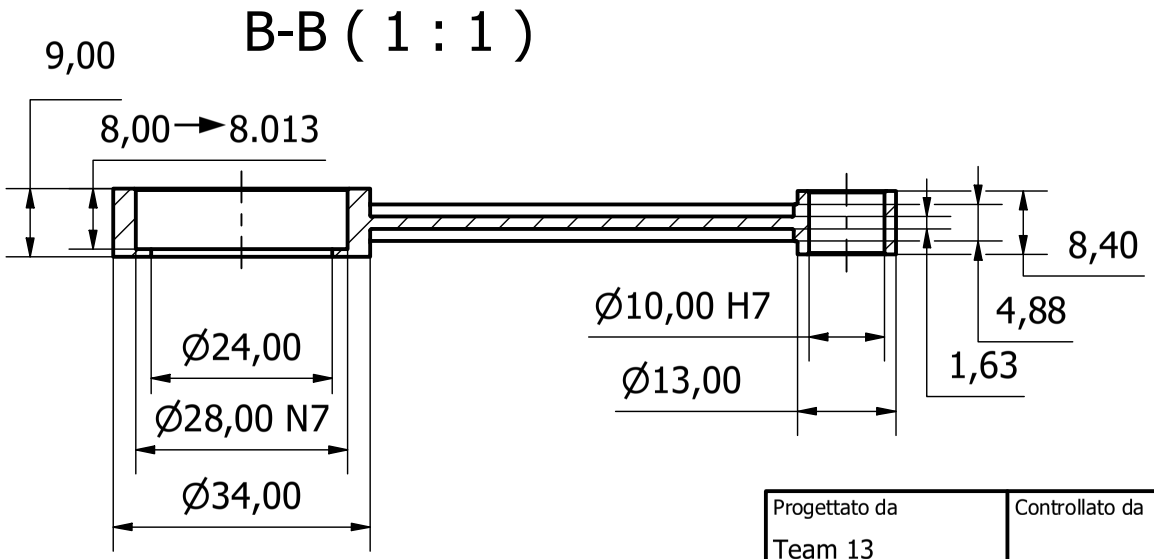

Dimensioni non quotate	
Oggetto	Definizione generale
Raccordi non quotati	R 0.2
Smussi non quotati	0.2 x 45°

Progettato da	Controllato da	Approvato da	Data		Data	
Team 13					03/01/2022	
		Rod		Edizione 1	Scala 1:1	

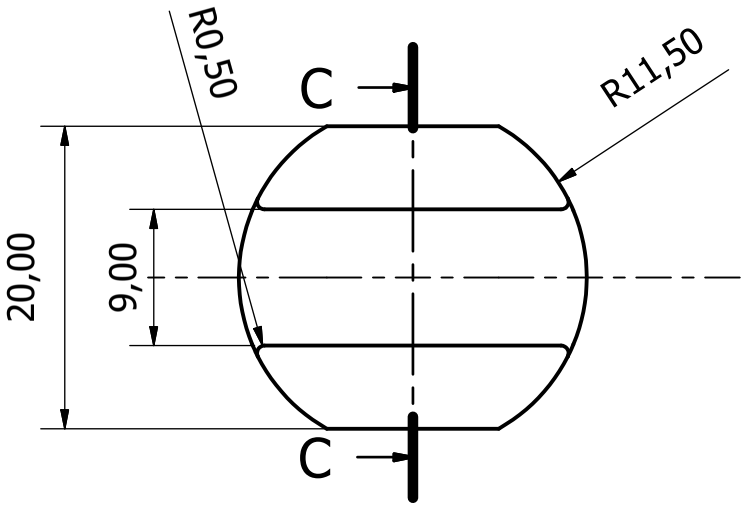

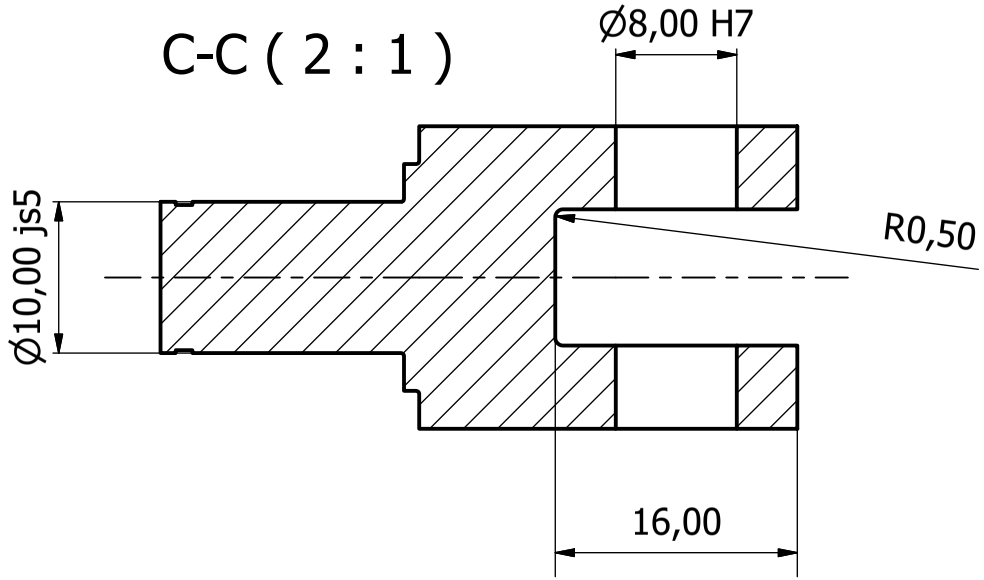

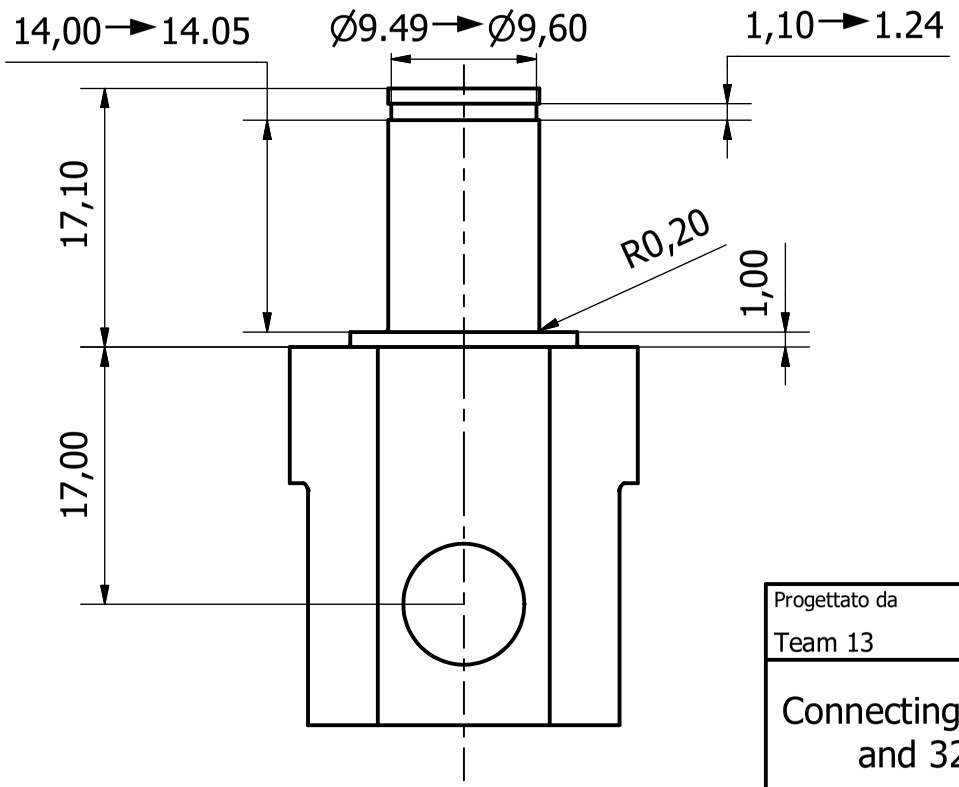

Dimensioni non quotate	
Oggetto	Definizione generale
Raccordi non quotati	R 0.2

Progettato da	Controllato da	Approvato da	Data		Data	
Team 13					03/01/2022	
Connecting element between rod and 3200 ATN9 bearing				rod connector	Edizione	Scala 2:1

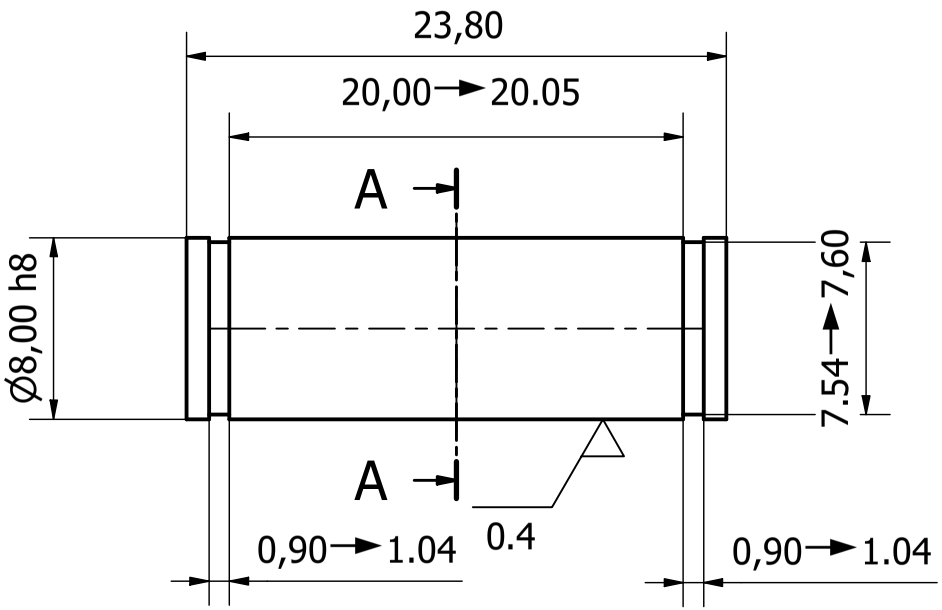

A-A (3 : 1)

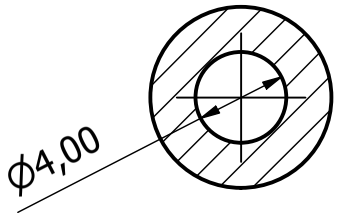

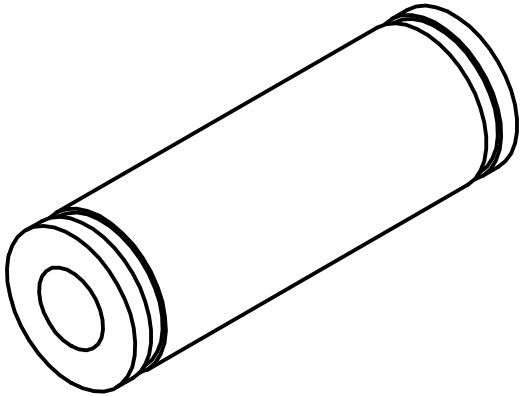

Progettato da	Controllato da	Approvato da	Data		Data	
Team 13					03/01/2022	
Connecting pin between rod and rod connector				Spinotto	Edizione	Scala 3:1

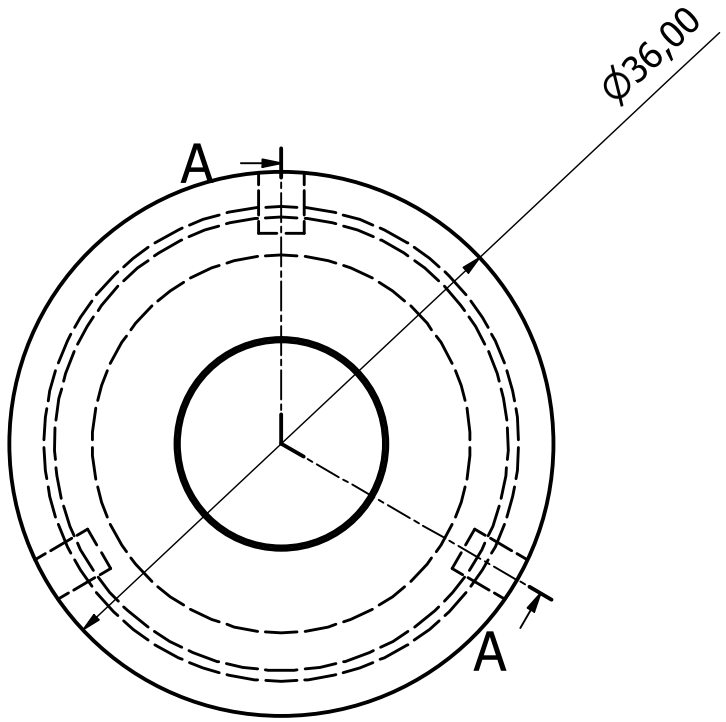

A-A (2 : 1)

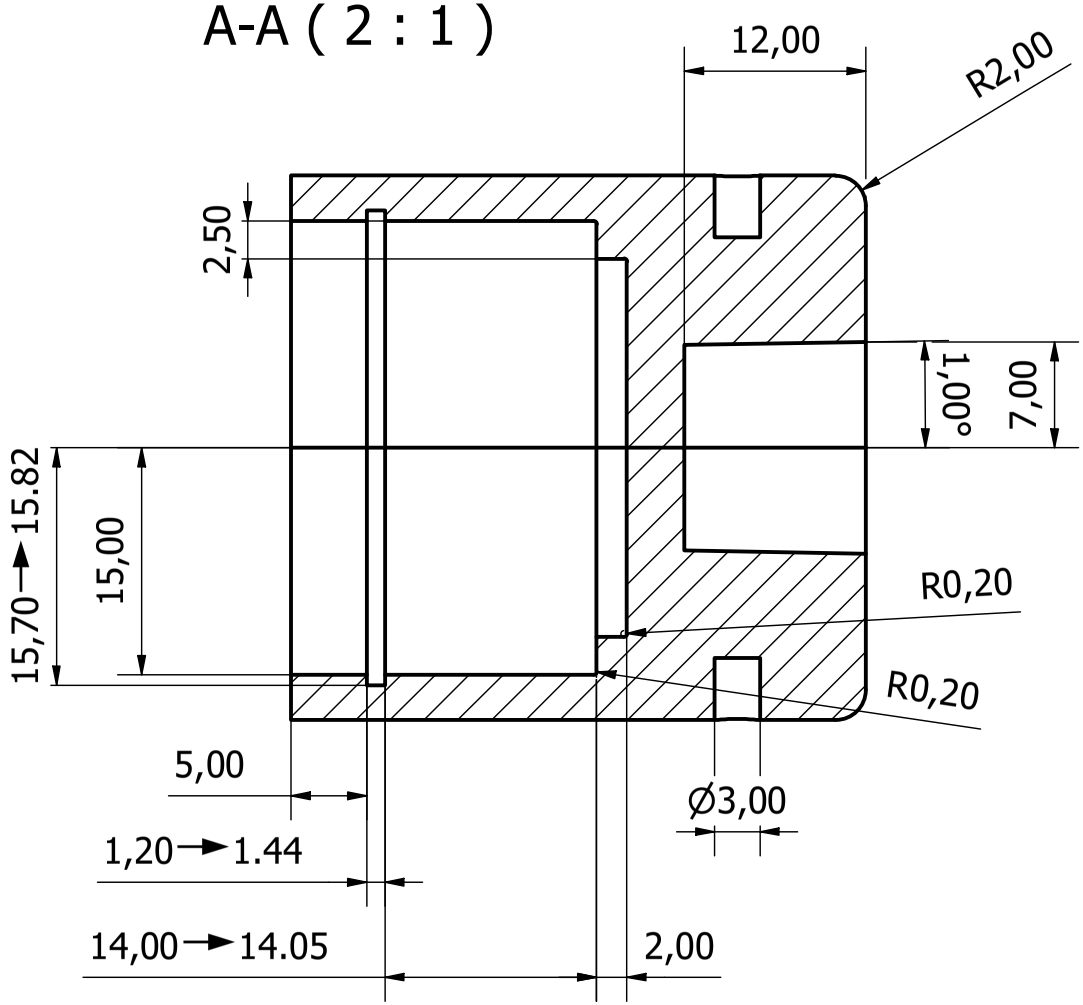

Progettato da	Controllato da	Approvato da	Data		Data	
Team 13					06/01/2022	
Follower of cam joint, attached to massage head			Piston			
			New_piston		Edizione	Scala 2:1

Free Body Diagram Analysis

$with(plots):$
$with(LinearAlgebra):$
$interface(rtablesize = 15):$

Closure equations

Solve the kinematics to link the angles of the mechanism

$crankrod := [lb = 0.08,\ lm = 0.006]:$
$driven := [theta_b, s];$

$$driven := [\theta_b, s] \tag{1.1}$$

$eq := +\ lb * \langle \cos(theta_b), \sin(theta_b) \rangle - lm * \langle \cos(\mathrm{Pi} - theta_m), \sin(\mathrm{Pi} - theta_m) \rangle\ - \langle s, 0 \rangle$

$$eq := \begin{bmatrix} lb \cos(\theta_b) + lm \cos(\theta_m) - s \\ lb \sin(\theta_b) - lm \sin(\theta_m) \end{bmatrix} \tag{1.2}$$

$sol := solve(convert(eq, list), driven):$
$soltheta_b := subs(crankrod, op(sol)[1]);$
$plot\left(rhs\left(soltheta_b \cdot \frac{180}{\mathrm{Pi}}\right), \theta_m = -\mathrm{Pi}..\mathrm{Pi}\right);$

$$soltheta_b := \theta_b = \arcsin(0.07500000000 \sin(\theta_m))$$

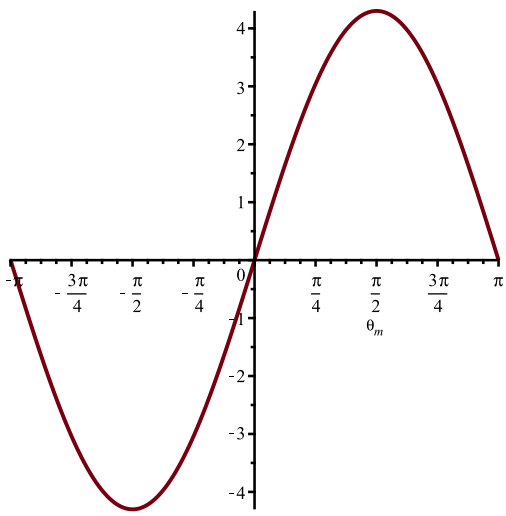

Plane Y-Z

Reaction forces

$qt_y := \frac{(q1_y - q0_y)}{L1} \cdot z;$

$$qt_y := \frac{(q1_y - q0_y)\, z}{L1} \tag{2.1.1}$$

$data := \{FA = 350,\ FR = 150, L_{head} = 75, L1 = 80, L2 = 25, L3 = 100,$

$$L4 = 6, \theta_m = \frac{\mathrm{Pi}}{2}, \mathrm{rho} = 2.7/10\text{^}9, Af = 28.866, \mathrm{omega} = 418.879 \Big\} :$$

$$\theta_b := \arcsin(0.07500000000 * \sin(\theta_m)) :$$

Rod centrifugal force contribution

$$qi := \frac{\mathrm{rho} \cdot Af \cdot x}{L3} \cdot \mathrm{omega}\text{^}2 \cdot L4 :$$

$$data_biella := [\mathrm{rho} = 2.7/10\text{^}9, Af = 28.866, \mathrm{omega} = 418.879, r = 6, L3 = 80] : \quad \#\, g/cm\text{^}3\,,\ mm2\,,\ rad/s\,,\ mm$$

$$Q_y := \int_0^{L3} qi \, \mathrm{d}x;$$

$$\#Q_y := subs(data_biella, Q);$$

$$x_Q := \frac{\int_0^{L3} qi \cdot x \, \mathrm{d}x}{\int_0^{L3} qi \, \mathrm{d}x};$$

$$x_Q_s := subs(data_biella, x_Q) :$$

$$Q_y := \frac{\rho\, Af\, L3\, \omega^2\, L4}{2}$$

$$x_Q := \frac{2\, L3}{3} \qquad \textbf{(2.1.2)}$$

$$follower := op\left(convert\left(\left[\begin{array}{c} FR - \int_0^{L1} (q0_y + qt_y)\, \mathrm{d}z + ray \\ ray \cdot L1 - \int_0^{L1} (q0_y + qt_y) \cdot z \, \mathrm{d}z + ma_x \\ raz = FA \end{array}\right], list\right)\right) : \langle \% \rangle :$$

$$connector := op\left(convert\left(\left[\begin{array}{c} rby = ray \\ rbz = FA \\ -ma_x + ray \cdot L2 \end{array}\right], list\right)\right) : \langle \% \rangle :$$

$$rod := op\left(convert\left(\left[\begin{array}{c} -rby + rcy + Q_y \cdot \cos(\theta_b) = 0 \\ rbz - rcz + Q_y \cdot \sin(\theta_b) = 0 \\ -\frac{Q_y}{3} \cdot L3 + rby \cdot L3 \cdot \cos(\theta_b) - rbz \cdot L3 \cdot \sin(\theta_b) = 0 \end{array}\right], list\right)\right) : \langle \% \rangle :$$

$$hub := op\left(convert\left(\left[\begin{array}{c} rcz = rdz \\ rcy = rdy \\ rcz \cdot \sin(\theta_m) \cdot L4 + rcy \cdot \cos(\theta_m) \cdot L4 = md_x \end{array}\right], list\right)\right) : \langle \% \rangle :$$

Solve for reaction forces

$$reaction_forces := simplify((op(solve([follower, connector, rod, hub], [q0_y, q1_y, ray, rby, rcy, rdy, rcz, raz, rbz, rdz, ma_x, md_x]))))) :$$

$$subs(data, reaction_forces) : \langle \% \rangle;$$

$$\left[\begin{array}{c} q0_y = 6.158499022 \\ q1_y = -1.716111416 \\ ray = 27.69550412 \\ rby = 27.69550412 \\ rcy = 23.60455668 \\ rdy = 23.60455668 \\ rcz = 350.3076877 \\ raz = 350 \\ rbz = 350 \\ rdz = 350.3076877 \\ ma_x = 692.3876031 \\ md_x = 2101.846126 \end{array}\right] \quad \textbf{(2.1.3)}$$

Internal actions

$$V1y := simplify\left(subs\left(FR - \int_0^z (q0_y + qt_y)\, dz\right)\right) :$$

$$M1x := \int_0^z V1y\, dz :$$

$$M1x := subs(reaction_forces, M1x) :$$
$$V1y := subs(reaction_forces, V1y) :$$
$$N1 := -FA :$$

$$V2y := subs(reaction_forces, -ray) :$$
$$M2x := subs(reaction_forces, -ray \cdot z + ma_x) :$$
$$N2 := subs(reaction_forces, -FA) :$$

$$N3 := -(rbz \cos(\theta_b) + rby \sin(\theta_b)) :$$
$$N3 := subs(reaction_forces, N3) :$$

$$V3y := -rby \cdot \cos(\theta_b) + rbz \cdot \sin(\theta_b) + \int_0^z qi\, dx :$$

$$M3x := \int_0^z V3y\, dz :$$

$$V3y := subs(reaction_forces, V3y) :$$
$$M3x := subs(reaction_forces, M3x) :$$

$$V4y := subs(reaction_forces, + rcy \cdot \cos(\theta_m) + rcz \cdot \sin(\theta_m)) :$$

$$M4x := \int_0^z V4y \, dx :$$

$$\#M4 := subs\left(reaction_forces, + rbz \cdot z \sin(\theta_m) + rby \cos(\theta_m) \cdot z\right) :$$
$$N4 := subs\left(reaction_forces, -rcz \cos(\theta_m) - rcy \sin(\theta_m)\right) :$$
$$M4 := subs(reaction_forces, M4) :$$
$$N4 := subs(reaction_forces, N4) :$$

Z-X plane

Reaction forces

$$qt := \frac{(q1_x - q0_x)}{L1} \cdot z :$$

$$follower := op\left(convert\left(\left[\begin{array}{c} raz = FA \\ -FR - rax + \int_0^{L1} \left(q0_x + qt\right) dz \\ rax \cdot L1 - \int_0^{L1} (q0_x + qt) \cdot z dz + may \end{array}\right], list\right)\right) : \langle \% \rangle :$$

$$connector := op\left(convert\left(\left[\begin{array}{c} rbz = raz \\ rax = 0 \\ -may + mby \end{array}\right], list\right)\right) : \langle \% \rangle :$$

$$rod := op\left(convert\left(\left[\begin{array}{c} 0 = 0 \\ -rcz + rbz + Q_y \cdot \sin(\theta_b) \\ mcy = mby \end{array}\right], list\right)\right) : \langle \% \rangle :$$

$$hub := op\left(convert\left(\left[\begin{array}{c} 0 = 0 \\ rdz = rcz \\ mdy = mcy \end{array}\right], list\right)\right) : \langle \% \rangle :$$

Solve for reaction forces

$$reaction_forces := op\left(solve\left([follower, connector, rod, hub], [q0_x, q1_x, raz, rax, rbz, mby, rcz, mcy, rdz, mdy]\right)\right) :$$

Internal actions

$$V1x := simplify\left(FR - \int_0^z (q0_x + qt) \, dz\right);$$

$$M1y := \int_0^z V1x \, dz;$$
$$M1y := subs(reaction_forces, M1y);$$
$$V1x := subs(reaction_forces, V1x);$$

$$M2y := subs(reaction_forces, may);$$

$M3y := subs(reaction_forces, mby);$

$M4y := subs(reaction_forces,\ mcy);$

$$V1x := \frac{\left(-2\,q0_x\,z + 2\,FR\right) L1 + \left(-q1_x + q0_x\right) z^2}{2\,L1}$$

$$M1y := \frac{\left(-q1_x + q0_x\right) z^3}{6\,L1} - \frac{z^2\,q0_x}{2} + FRz$$

$$M1y := \frac{\left(\frac{2.\,(FRL1 - 3.\,may)}{L1^2} + \frac{2.\,(2.\,FRL1 - 3.\,may)}{L1^2}\right) z^3}{6\,L1} - \frac{1.000000000\,z^2\,(2.\,FRL1 - 3.\,may)}{L1^2} + FRz$$

$$V1x := \frac{\left(-\frac{4.\,(2.\,FRL1 - 3.\,may)\,z}{L1^2} + 2\,FR\right) L1 + \left(\frac{2.\,(FRL1 - 3.\,may)}{L1^2} + \frac{2.\,(2.\,FRL1 - 3.\,may)}{L1^2}\right) z^2}{2\,L1}$$

$$M2y := may$$

$$M3y := may$$

$$M4y := may \qquad \textbf{(3.2.1)}$$

Castigliano's theorem to calculate the unknown (here we are assuming all parts with same E*I)

$may := X:$

$$iperstatic := simplify\left(\int_0^{L1} M1y \cdot \frac{\partial}{\partial X}(M1y)\,\mathrm{d}z + \int_0^{L2} M2y \cdot \frac{\partial}{\partial X}(M2y)\,\mathrm{d}z + \int_0^{L3} M3y \cdot \frac{\partial}{\partial X}(M3y)\,\mathrm{d}z + \int_0^{L4} M4y \cdot \frac{\partial}{\partial X}(M4y)\,\mathrm{d}z\right);$$

$evalf(subs(data,\ solve(iperstatic, [X]))\,);$

$data := [\ op(data), op(op(\%))\,]:$

$subs(data, reaction_forces) : \langle\%\rangle$

$$iperstatic := (0.371428571\,L1 + L2 + L3 + L4)\,X + 0.030952381\,FRL1^2$$

$$[[X = -184.8888892]]$$

$$\begin{bmatrix} q0_x = 7.673333334 \\ q1_x = -3.923333334 \\ raz = 350 \\ rax = 0. \\ rbz = 350 \\ mby = -184.8888892 \\ rcz = 350.3076877 \\ mcy = -184.8888892 \\ rdz = 350.3076877 \\ mdy = -184.8888892 \end{bmatrix} \qquad \textbf{(3.2.2)}$$

Internal actions plot

$n1 := plot(subs(data, N1), z = 0 .. subs(data, L1), color = \text{"DodgerBlue"}, gridlines = true, title = [\text{"N Follower"}], labels = [mm, N]) :$
$n2 := plot(subs(data, N2), z = 0 .. subs(data, L2), color = \text{"Crimson"}, gridlines = true, title = [\text{"N Rod Connector"}], labels = [mm, N]) :$
$n3 := plot(subs(data, N3), z = 0 .. subs(data, L3), color = \text{"Green"}, gridlines = true, title = [\text{"N Rod"}], labels = [mm, N]) :$
$n4 := plot(subs(data, N4), z = 0 .. subs(data, L4), color = \text{"Brown"}, gridlines = true, title = [\text{"N Motor Hub"}], labels = [mm, N]) :$

$v1 := plot(subs(data, V1y), z = 0 .. subs(data, L1), color = \text{"DodgerBlue"}, gridlines = true, title = [\text{"Vy Follower"}], labels = [mm, N]) :$
$v2 := plot(subs(data, V2y), z = 0 .. subs(data, L2), color = \text{"Crimson"}, gridlines = true, title = [\text{"Vy Rod Connector"}], labels = [mm, N]) :$
$v3 := plot(subs(data, V3y), z = 0 .. subs(data, L3), color = \text{"Green"}, gridlines = true, title = [\text{"Vy Rod"}], labels = [mm, N]) :$
$v4 := plot(subs(data, V4y), z = 0 .. subs(data, L4), color = \text{"Brown"}, gridlines = true, title = [\text{"Vy Motor Hub"}], labels = [mm, N]) :$

$\#v1x := plot(subs(data, V1x), z = 0 .. subs(data, L1), color = \text{"DodgerBlue"}, gridlines = true, title = [\text{"Follower } XShear\text{"}]) :$

$m1x := plot(subs(data, M1x), z = 0 .. subs(data, L1), color = \text{"DodgerBlue"}, gridlines = true, title = [\text{"Mx Follower"}], labels = [mm, Nmm]) :$
$m2x := plot(subs(data, M2x), z = 0 .. subs(data, L2), color = \text{"Crimson"}, gridlines = true, title = [\text{"Mx Rod Connector"}], labels = [mm, Nmm]) :$
$m3x := plot(subs(data, M3x), z = 0 .. subs(data, L3), color = \text{"Green"}, gridlines = true, title = [\text{"Mx Rod"}], labels = [mm, Nmm]) :$
$m4x := plot(subs(data, M4x), z = 0 .. subs(data, L4), color = \text{"Brown"}, gridlines = true, title = [\text{"Mx Motor Hub"}], labels = [mm, Nmm]) :$

$m1y := plot(subs(data, M1y), z = 0 .. subs(data, L1), color = \text{"DodgerBlue"}, gridlines = true, title = [\text{"My Follower"}], labels = [mm, Nmm]) :$
$m2y := plot(subs(data, M2y), z = 0 .. subs(data, L2), color = \text{"Crimson"}, gridlines = true, title = [\text{"My Connector"}], labels = [mm, Nmm]) :$
$m3y := plot(subs(data, M3y), z = 0 .. subs(data, L3), color = \text{"Green"}, gridlines = true, title = [\text{"My Rod"}], labels = [mm, Nmm]) :$
$m4y := plot(subs(data, M3y), z = 0 .. subs(data, L4), color = \text{"Green"}, gridlines = true, title = [\text{"My Motor Hub"}], labels = [mm, Nmm]) :$

$display(Matrix([n1, n2]), size = [200, 300]);$
$display(Matrix([n3, n4]), size = [200, 300]) ;$

$display(Matrix([v1, v2]), size = [200, 300]);$
$display(Matrix([m1x, m2x]), size = [200, 300]);$

$display(Matrix([v3, v4]), size = [200, 300]);$
$display(Matrix([m3x, m4x]), size = [200, 300]);$

$display(Matrix([m1y, m2y]), size = [200, 300]);$
$display(Matrix([m3y, m4y]), size = [200, 300]);$

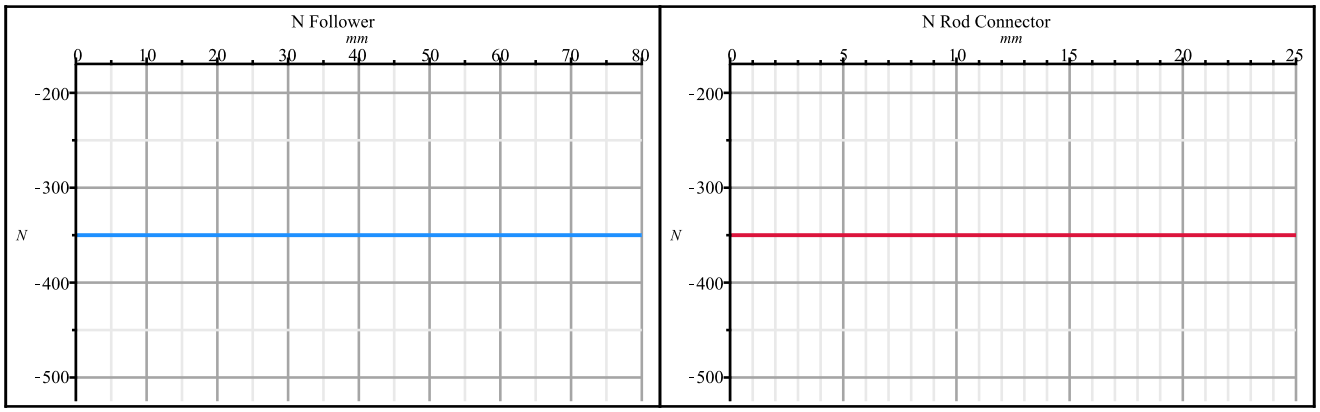

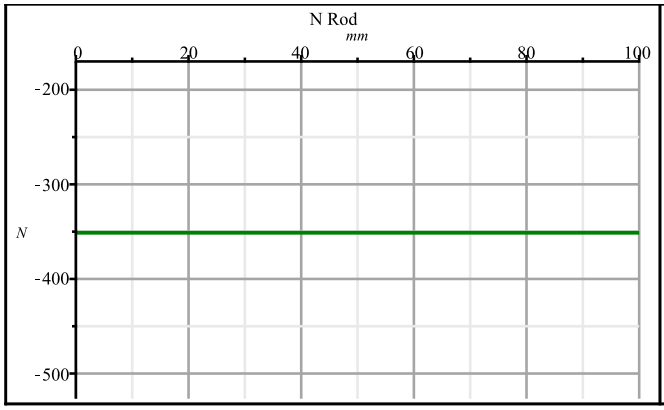
N Rod
mm
0
20
40
60
80
100
-200
-300
N
-400
-500

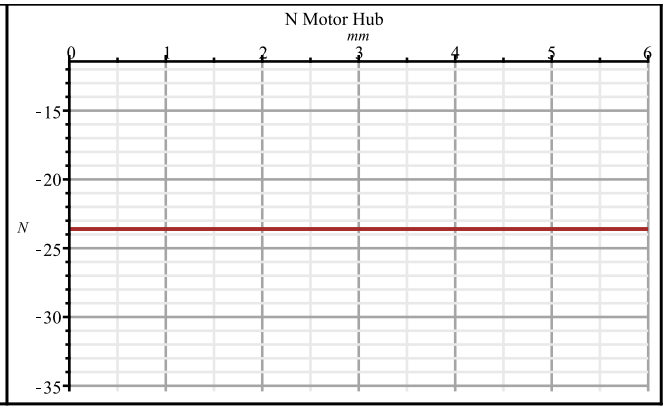
N Motor Hub
mm
0
1
2
3
4
5
6
-15
-20
N
-25
-30
-35

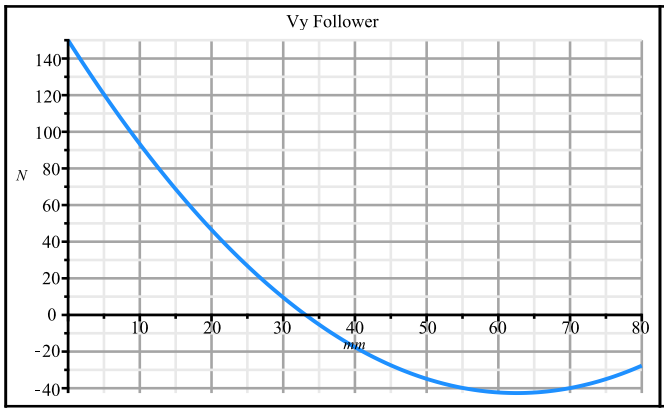
Vy Follower
140
120
100
N
80
60
40
20
0
-20
-40
10
20
30
40
50
60
70
80
mm

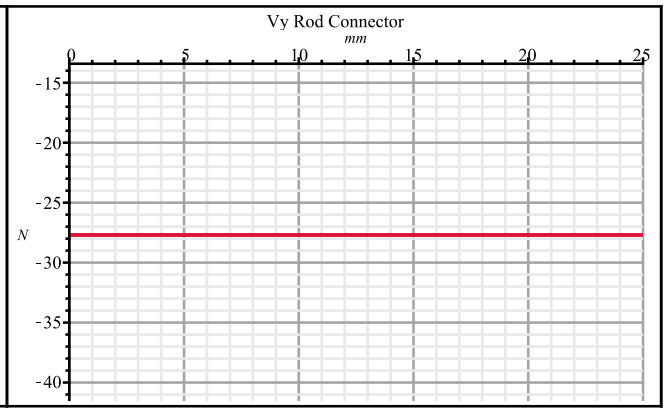
Vy Rod Connector
mm
0
5
10
15
20
25
-15
-20
-25
N
-30
-35
-40

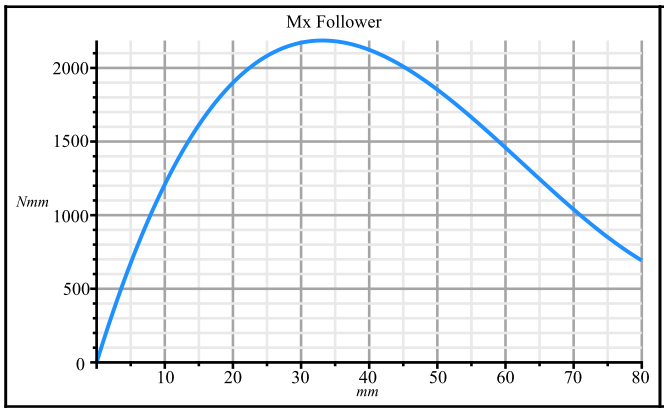
Mx Follower
2000
1500
Nmm
1000
500
0
10
20
30
40
50
60
70
80
mm

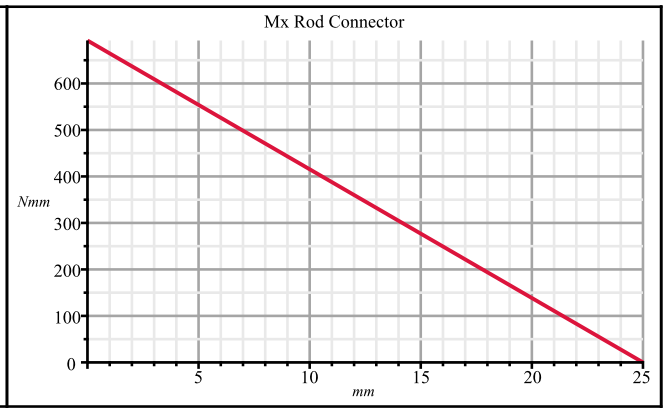
Mx Rod Connector
600
500
400
Nmm
300
200
100
0
5
10
15
20
25
mm

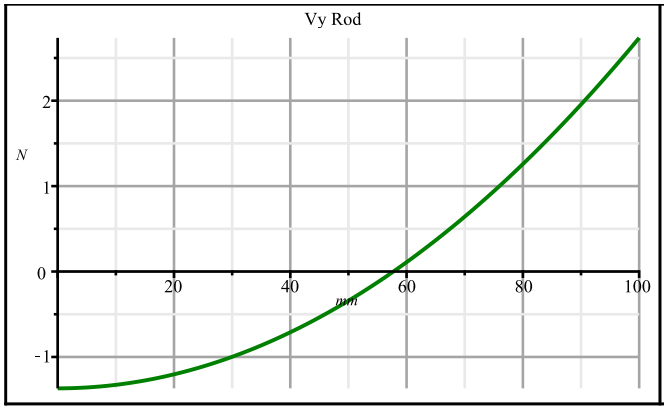
Vy Rod
N
mm

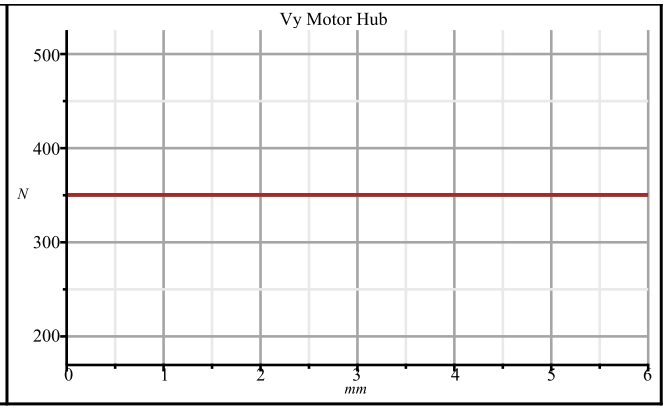
Vy Motor Hub
N
mm

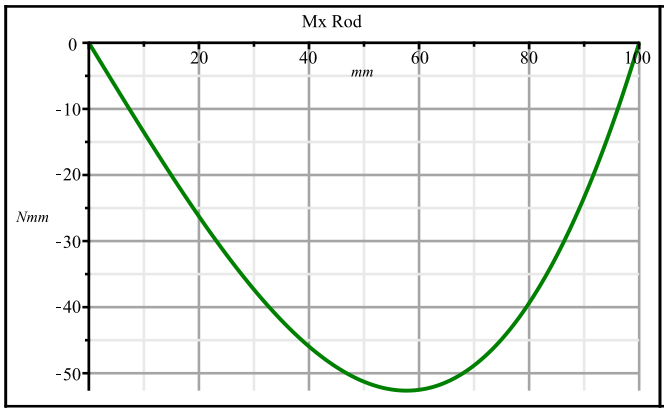
Mx Rod
Nmm
mm

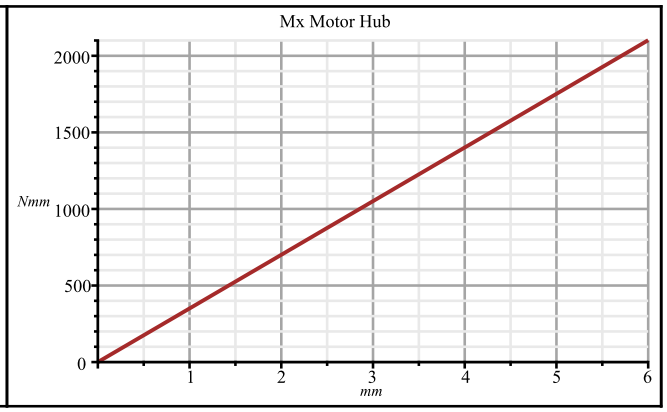
Mx Motor Hub
Nmm
mm

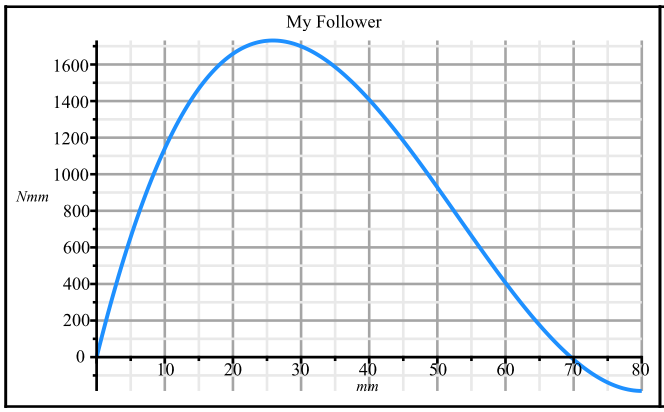
My Follower
Nmm
mm

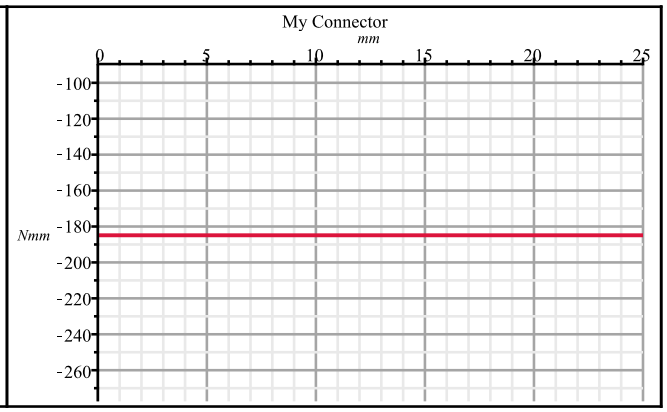
My Connector
mm
Nmm

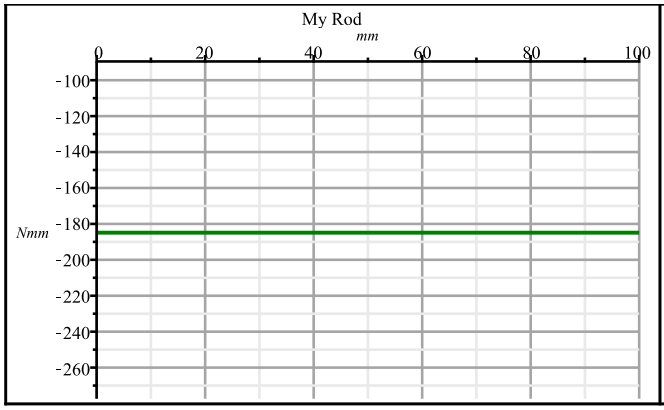
My Rod
mm
0
20
40
60
80
100
-100
-120
-140
-160
-180
-200
-220
-240
-260
Nmm

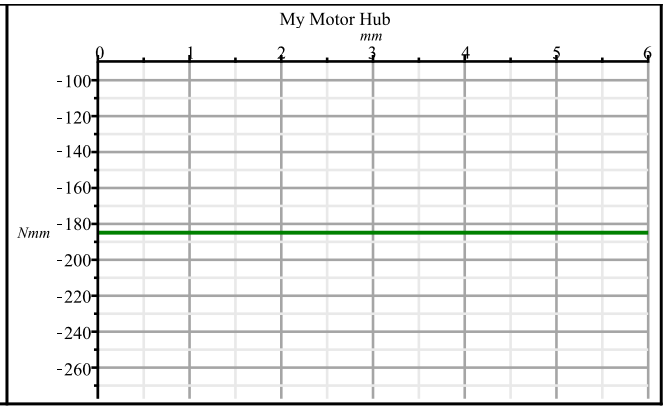
My Motor Hub
mm
0
1
2
3
4
5
6
-100
-120
-140
-160
-180
-200
-220
-240
-260
Nmm

References

[1] Shigley, Joseph Edward. Shigley's mechanical engineering design. Tata McGraw-Hill Education, 2011.

[2] Ullman, David G. The Mechanical Design Process, Fourth Edition. Tata McGraw-Hill series in mechanical engineering, 2010.

Appendix

SKF Bearing Select Report 1.3-168

February 05, 2022

1. Abstract

Calculation overview

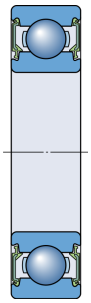

Deep groove ball bearing

■ SKF Explorer ☆ Popular item

	Bearing rating life		Grease	Static safety factor	Frictional moment	Power loss
Designation	Basic	SKF life	Catalogue grease life		Total	
	L_{10h} (h)	L_{10mh} (h)	L_{10} (h)	S_0	M (Nmm)	P_{loss} (W)
☆ ■ 6001-2RSL	15300	> 2x10^5	86300	6.74	5.49	2.3

* SKF rating life (L_{10mh}) for steel-steel bearings; GBLM load based life (L_{10GMh}) for hybrid bearings

Consideration

For rating life results above 100000 hours, other failure modes than those included in the current rating life models will dominate and limit the life of the bearing.

This report was produced with SKF Bearing Select software. Please note the limited warranty, shown at the bottom of the last page of this report
® SKF is a registered trademark of the SKF Group. © SKF Group 2019.

2. Input

2.1. Bearing data

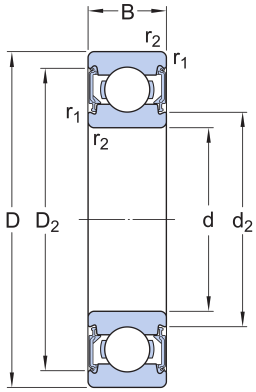

		Principal dimensions			Basic load ratings		Fatigue load limit	Speed ratings		Clearance class
Designation	Bearing type				Dynamic	Static		Reference	Limiting	
		d (mm)	D (mm)	B (mm)	C (kN)	C_0 (kN)	P_u (kN)	n_{ref} (r/min)	n_{lim} (r/min)	
☆ ■ 6001-2RSL	Deep groove ball bearing	12.0	28.0	8.0	5.4	2.36	0.1	60000.0	30000.0	Normal

2.2. Loads, Speed and Temperature

Shaft orientation	Horizontal
Rotating ring	Outer ring rotation

	Forces		Speed	Temperature		Case weight
	Radial (F_r) (kN)	Axial (F_a) (kN)	(r/min)	Inner ring (°C)	Outer ring (°C)	
LC1	0.35	0.0	4000.0	40	40	1

Maximum temperature is used for calculating the actual viscosity, kappa, a_{SKF} and SKF rating life.

Mean temperature is used for calculating bearing friction and power loss.

2.3. Lubrication

	Lubricant	Effective EP additives	Contamination	
Designation	Name		Method	Cleanliness / Factor
☆ ■ 6001-2RSL	LHT23	False	Detailed guidelines	High cleanliness

This report was produced with SKF Bearing Select software. Please note the limited warranty, shown at the bottom of the last page of this report
® SKF is a registered trademark of the SKF Group. © SKF Group 2019.

2.4. Fits and tolerances

	Requirements		Calculated interference	Include Smoothing	Easy axial displacement of inner ring on shaft
Designation	Guidance	Load direction rotating ring			
6001-2RSL	True	constant	True	True	True

3. Results

3.1. Loads & static safety

	Load ratio	Static safety factor	Equivalent dynamic load	Equivalent static load
Designation	C/P	S_0	P (kN)	P_0 (kN)
6001-2RSL	15.43	6.74	0.35	0.35

3.2. Bearing minimum load

	Reaction forces		Minimum load	
Designation	Radial	Axial		Requirements
	F_r (kN)	F_a (kN)	F_{rm} (kN)	met?
6001-2RSL	0.35	0.0	0.0227	yes

3.3. Adjusted reference speed

	Adjusted reference speed	Adjustment factors	
Designation		For bearing load P	For oil viscosity
	n_{ar} (r/min)	f_p	f_v
6001-2RSL	78400	0.88	1.49

3.4. Lubrication conditions

	Operating viscosity			Viscosity ratio
Designation	Actual	Rated	Rated @ 40 °C	
	ν (mm^2/s)	$ν_1$ (mm^2/s)	$ν_{ref}$ (mm^2/s)	K
6001-2RSL	26.9	13.4	13.4	2.01

This report was produced with SKF Bearing Select software. Please note the limited warranty, shown at the bottom of the last page of this report
® SKF is a registered trademark of the SKF Group. © SKF Group 2019.

3.5. Grease life and relubrication interval

	Catalogue grease life	Speed factor
Designation		Speed x mean diameter
	L_{10} (h)	nd_m (mm/min)
☆ ■ 6001-2RSL	86300	112000

3.6. Bearing rating life

	Bearing rating life		SKF life modification factor	Contamination factor
Designation	Basic	SKF		
	L_{10h} (h)	L_{10mh} (h)	a_{skf}	η_c
☆ ■ 6001-2RSL	15300	> 2x10^5	13.56	0.54

* SKF rating life (L_{10mh}) for steel-steel bearings; GBLM load based life (L_{10GMh}) for hybrid bearings

Consideration

For rating life results above 100000 hours, other failure modes than those included in the current rating life models will dominate and limit the life of the bearing.

3.7. Bearing friction & power loss

	Frictional moment		Friction sources				Power loss
Designation	Total	At start 20-30°C and zero speed	Rolling	Sliding	Seals	Drag loss	
	M (Nmm)	M_{start} (Nmm)	M_{rr} (Nmm)	M_{sl} (Nmm)	M_{seal} (Nmm)	M_{drag} (Nmm)	P_{loss} (W)
☆ ■ 6001-2RSL	5.49	5.23	3.23	1.49	0.76	0	2.3

3.8. Bearing frequencies

	Rotational frequencies				Frequency of over-rolling		
Designation	Inner ring	Outer ring	Rolling element set & cage	Rolling element about its axis	Point on inner ring	Point on outer ring	Rolling element
	f_i (Hz)	f_e (Hz)	f_c (Hz)	f_r (Hz)	f_{ip} (Hz)	f_{ep} (Hz)	f_{rp} (Hz)
☆ ■ 6001-2RSL	0.0	66.667	41.27	132.061	330.16	203.173	264.121

This report was produced with SKF Bearing Select software. Please note the limited warranty, shown at the bottom of the last page of this report
® SKF is a registered trademark of the SKF Group. © SKF Group 2019.

3.9. Fits and tolerances

Note
Typically, it is not sufficient to use an interference fit alone to axially locate a bearing ring on a cylindrical seat.

3.9.1. Recommended tolerance class

	Tolerance Class	
Designation	Shaft	Housing
☆ ■ 6001-2RSL	g6	N7

Consideration
The recommendation for the tolerance classes is based on the load case with the highest equivalent dynamic load.

Consideration
Valid for solid steel shaft and split or non-split cast iron or steel housings.

3.9.2. Tolerances

	Shaft outer diameter		Bearing bore		Bearing outer diameter		Housing bore		Smoothing	
Designation	Minimum	Maximum	Minimum	Maximum	Minimum	Maximum	Minimum	Maximum	Shaft and bearing bore	Bearing outer ring and housing
	(µm)	(µm)	(µm)	(µm)	(µm)	(µm)	(µm)	(µm)	(µm)	(µm)
☆ ■ 6001-2RSL	-17	-6	-8	0	-9	0	-28	-7	7	14

Consideration
For the tolerances calculation, the normal tolerance for the bearing bore and outer diameter is used.

3.9.3. Fits, Probable Interference (+) / Clearance (-)

	Shaft			Housing		
Designation	Probable minimum	Middle	Probable maximum	Probable minimum	Middle	Probable maximum
	(µm)	(µm)	(µm)	(µm)	(µm)	(µm)
☆ ■ 6001-2RSL	-21	-15	-8	-12	-1	10

LIMITED WARRANTY : The SKF Bearing Select software tool of the SKF Company supports the calculation and selection of bearings.
This software is provided 'as is' with out any warranty of any sort, implicitly as well as explicitly.
Please note that the obtained results can be affected by many external parameters and/or the quality of the assumptions taken into account.
The results obtained using this software must be validated by the user who accepts the fact that the use of this software and the exploitation of the obtained results are under the user's entire and sole responsibility.
® SKF is a registered trademark of the SKF Group. © SKF Group 2019.

February 05, 2022

1. Abstract

Calculation overview

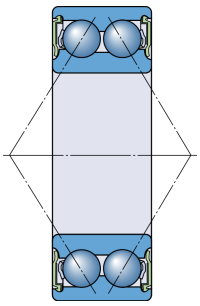

Angular contact ball bearing

SKF Explorer ☆ Popular item

	Bearing rating life		Grease	Static safety factor	Frictional moment	Power loss
Designation	Basic	SKF life	Catalogue grease life		Total	
	L_{10h} (h)	L_{10mh} (h)	L_{10} (h)	S_0	M (Nmm)	P_{loss} (W)
☆ 3200 A-2R S1TN9/MT33	72200	> 2x10^5	100000	15.2	23.6	2.5

* SKF rating life (L_{10mh}) for steel-steel bearings; GBLM load based life (L_{10GMh}) for hybrid bearings

Consideration

For rating life results above 100000 hours, other failure modes than those included in the current rating life models will dominate and limit the life of the bearing.

This report was produced with SKF Bearing Select software. Please note the limited warranty, shown at the bottom of the last page of this report
® SKF is a registered trademark of the SKF Group. © SKF Group 2019.

2. Input

2.1. Bearing data

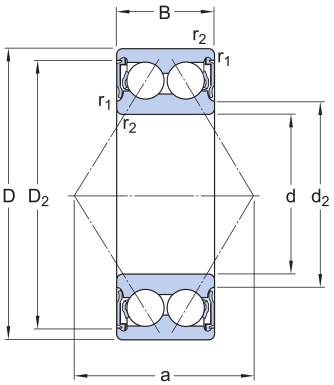

		Principal dimensions			Basic load ratings		Fatigue load limit	Speed ratings	
Designation	Bearing type				Dynamic	Static		Reference	Limiting
		d (mm)	D (mm)	B (mm)	C (kN)	C_0 (kN)	P_u (kN)	n_{ref} (r/min)	n_{lim} (r/min)
☆ 3200 A-2RS1TN9/MT33	Angular contact ball bearing	10.0	30.0	14.0	7.61	4.3	0.183		17000.0

2.2. Loads, Speed and Temperature

Shaft orientation	Horizontal
Rotating ring	Inner ring rotation

	Forces		Speed	Temperature		Case weight
	Radial (F_r) (kN)	Axial (F_a) (kN)	(r/min)	Inner ring (°C)	Outer ring (°C)	
LC1	0.052	0.35	1000.0	40	40	1

Maximum temperature is used for calculating the actual viscosity, kappa, a_{SKF} and SKF rating life.

Mean temperature is used for calculating bearing friction and power loss.

2.3. Lubrication

	Lubricant	Effective EP additives	Contamination	
Designation	Name		Method	Cleanliness / Factor
☆ 3200 A-2RS1TN9/MT33	MT33	False	Detailed guidelines	High cleanliness

This report was produced with SKF Bearing Select software. Please note the limited warranty, shown at the bottom of the last page of this report
® SKF is a registered trademark of the SKF Group. © SKF Group 2019.

2.4. Fits and tolerances

	Requirements		Calculated interference	Include Smoothing	Thermal Shaft Expansion
Designation	Guidance	Load direction rotating ring			
☆ 3200 A-2RS1TN9/MT33	True	constant	True	True	False

3. Results

3.1. Loads & static safety

	Load ratio	Static safety factor	Equivalent dynamic load	Equivalent static load
Designation	C/P	S_0	P (kN)	P_0 (kN)
☆ 3200 A-2RS1TN9/MT33	16.3	15.2	0.47	0.283

3.2. Bearing minimum load

	Reaction forces		Minimum load	
Designation	Radial	Axial		Requirements
	F_r (kN)	F_a (kN)	F_{rm} (kN)	met?
☆ 3200 A-2RS1TN9/MT33	0.052	0.35	0.0517	yes

3.3. Lubrication conditions

	Operating viscosity			Viscosity ratio
Designation	Actual	Rated	Rated @ 40 °C	
	ν (mm^2/s)	$ν_1$ (mm^2/s)	$ν_{ref}$ (mm^2/s)	K
☆ 3200 A-2RS1TN9/MT33	99.9	26.9	26.9	3.7

3.4. Grease life and relubrication interval

	Catalogue grease life	Speed factor
Designation		Speed x mean diameter
	L_{10} (h)	nd_m (mm/min)
☆ 3200 A-2RS1TN9/MT33	100000	20000

This report was produced with SKF Bearing Select software. Please note the limited warranty, shown at the bottom of the last page of this report
® SKF is a registered trademark of the SKF Group. © SKF Group 2019.

3.5. Bearing rating life

	Bearing rating life		SKF life modification factor	Contamination factor
Designation	Basic	SKF		
	L_{10h} (h)	L_{10mh} (h)	a_{skf}	η_c
☆ 3200 A-2RS1TN9/MT33	72200	> 2x10^5	50.0	0.75

* SKF rating life (L_{10mh}) for steel-steel bearings; GBLM load based life (L_{10GMh}) for hybrid bearings

Consideration

For rating life results above 100000 hours, other failure modes than those included in the current rating life models will dominate and limit the life of the bearing.

3.6. Bearing friction & power loss

	Frictional moment		Friction sources				Power loss
Designation	Total	At start 20-30°C and zero speed	Rolling	Sliding	Seals	Drag loss	
	M (Nmm)	M_{start} (Nmm)	M_{rr} (Nmm)	M_{sl} (Nmm)	M_{seal} (Nmm)	M_{drag} (Nmm)	P_{loss} (W)
☆ 3200 A-2RS1TN9/MT33	23.6	26.9	5.65	4.53	13.4	0	2.5

3.7. Bearing frequencies

	Rotational frequencies				Frequency of over-rolling		
Designation	Inner ring	Outer ring	Rolling element set & cage	Rolling element about its axis	Point on inner ring	Point on outer ring	Rolling element
	f_i (Hz)	f_e (Hz)	f_c (Hz)	f_r (Hz)	f_{ip} (Hz)	f_{ep} (Hz)	f_{rp} (Hz)
☆ 3200 A-2RS1TN9/MT33	16.667	0.0	6.615	33.511	80.413	52.92	67.022

This report was produced with SKF Bearing Select software. Please note the limited warranty, shown at the bottom of the last page of this report
® SKF is a registered trademark of the SKF Group. © SKF Group 2019.

3.8. Fits and tolerances

Note
Typically, it is not sufficient to use an interference fit alone to axially locate a bearing ring on a cylindrical seat.

3.8.1. Recommended tolerance class

	Tolerance Class	
Designation	Shaft	Housing
☆ 3200 A-2RS1TN9/MT33	js5	H8

Consideration
The recommendation for the tolerance classes is based on the load case with the highest equivalent dynamic load.

Consideration
Valid for solid steel shaft and split or non-split cast iron or steel housings.

3.8.2. Tolerances

	Shaft outer diameter		Bearing bore		Bearing outer diameter		Housing bore		Smoothing	
Designation	Minimum	Maximum	Minimum	Maximum	Minimum	Maximum	Minimum	Maximum	Shaft and bearing bore	Bearing outer ring and housing
	(µm)	(µm)	(µm)	(µm)	(µm)	(µm)	(µm)	(µm)	(µm)	(µm)
☆ 3200 A-2RS1TN9/MT33	-3	3	-8	0	-9	0	0	33	4	12

Consideration
For the tolerances calculation, the normal tolerance for the bearing bore and outer diameter is used.

3.8.3. Fits, Probable Interference (+) / Clearance (-)

	Shaft			Housing		
Designation	Probable minimum	Middle	Probable maximum	Probable minimum	Middle	Probable maximum
	(µm)	(µm)	(µm)	(µm)	(µm)	(µm)
☆ 3200 A-2RS1TN9/MT33	-5	0	5	-50	-33	-16

LIMITED WARRANTY : The SKF Bearing Select software tool of the SKF Company supports the calculation and selection of bearings.
This software is provided 'as is' with out any warranty of any sort, implicitly as well as explicitly.
Please note that the obtained results can be affected by many external parameters and/or the quality of the assumptions taken into account.
The results obtained using this software must be validated by the user who accepts the fact that the use of this software and the exploitation of the obtained results are under the user's entire and sole responsibility.
® SKF is a registered trademark of the SKF Group. © SKF Group 2019.

1. Abstract

Calculation overview

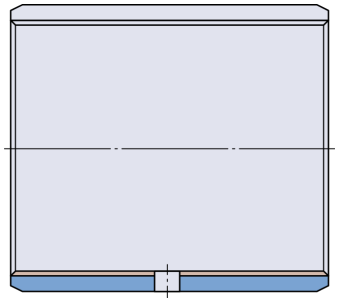

Composite Bushings

SKF Explorer ☆ Popular item

Designation	Basic rating life	
	G_h (h)	G (Oscillations)
PCM 081008 M	3530	847300000

2. Input

2.1. Bearing data

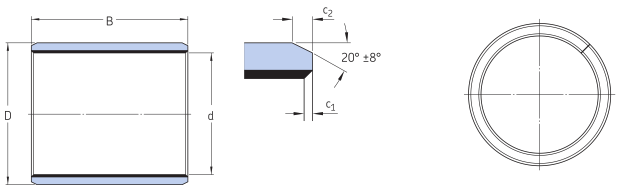

Designation	Bearing type	Principal dimensions			Basic load ratings	
		Bore	Outer diameter	Width	Dynamic	Static
		d (mm)	D (mm)	B (mm)	C (kN)	C_0 (kN)
PCM 081008 M	Composite bushings	8.0	10.0	8.0	7.65	16.0

This report was produced with SKF Bearing Select software. Please note the limited warranty, shown at the bottom of the last page of this report
® SKF is a registered trademark of the SKF Group. © SKF Group 2019.

2.2. Loads, frequency / speed or oscillation and Temperature

Input frequency / speed or oscillation	Frequency
Roughness, µm	0.4

		Forces	Frequency	Angle	Load direction	Temperature	Case weight
Designation	Load cases	Radial (kN)	min^{-1}	Half the angle of oscillation (°)		°C	
PCM 081008 M	LC1	0.351	4000	4.3	Stationary Load	30	1

3. Results

3.1. Bearing rating life

	Basic rating life	
Designation		
	G_h (h)	G (Oscillations)
PCM 081008 M	3530	847300000

3.2. Bearing rating life- pv Diagram

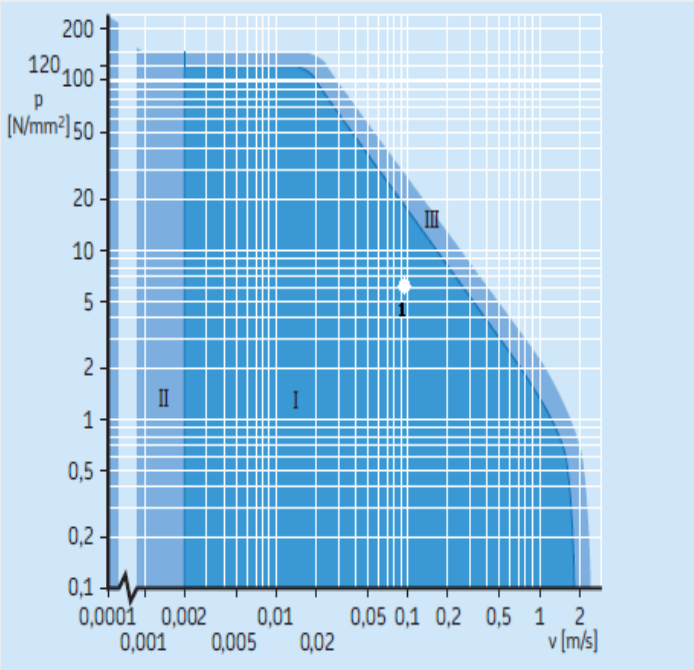

° Load case

I. Range when rating life equation is valid

II. Quasi-static range; before using the rating life equation, contact the SKF application engineering service

III. Possible range of use, e.g. with very good lubrication; before using the rating life equation, contact the SKF application engineering service for additional information

	Mean sliding velocity	Inner ring mean diameter	PV Range
Designation	v (m/s)	d_m (mm)	
PCM 081008 M	0.08008	8	I

This report was produced with SKF Bearing Select software. Please note the limited warranty, shown at the bottom of the last page of this report
® SKF is a registered trademark of the SKF Group. © SKF Group 2019.

3.3. Bearing rating life- Intermediate results

Designation	Specific	Factor depending on design & sliding contact surface
	p (N/mm)	K (N/mm)
PCM 081008 M	5.51	120.0

Designation	Correction factors				
	Load factor	Speed factor	Temperature factor	Surface roughness factor	Factor for type of load
	c_1	c_2	c_3	c_4	c_5
PCM 081008 M	1.316	1.0	0.888	0.701	1.0

LIMITED WARRANTY : The SKF Bearing Select software tool of the SKF Company supports the calculation and selection of bearings.
This software is provided 'as is' with out any warranty of any sort, implicitly as well as explicitly.
Please note that the obtained results can be affected by many external parameters and/or the quality of the assumptions taken into account.
The results obtained using this software must be validated by the user who accepts the fact that the use of this software and the exploitation of the obtained results are under the user's entire and sole responsibility.
® SKF is a registered trademark of the SKF Group. © SKF Group 2019.